Report Prepared by :

A. A. Sagüés
S.C. Kranc
R. H. Hoehne

INITIAL DEVELOPMENT OF METHODS FOR ASSESSING CONDITION OF POST-TENSIONED TENDONS OF SEGMENTAL BRIDGES

Contract # BC374

Final Report to Florida Department of Transportation

A. A. Sagüés and S. C. Kranc
Principal Investigators
Department of Civil and Environmental Engineering

University of South Florida
Tampa, FL, 33620
May 17, 2000

TABLE OF CONTENTS

NOTICE

EXECUTIVE SUMMARY

Examination of post tensioned tendons of the Niles Channel Bridge during Spring, 1999 indicated severe corrosion damage and strand separation near the anchorage points on two tendons. This investigation was conducted to determine the suitability of non destructive mechanical and electrical testing of tendons to detect strand failure.

Mechanical testing consisted of measuring the vibrational response of tendons to mechanical excitation, and using the results to estimate the tendon tension and stiffness. Comparisons among these values were used to identify indicators of possible distress. One of the indicators (relative difference in tension at opposite ends of the tendon) was strongest for a tendon previously known to have broken strands. Other indicators (low tension, low stiffness) may serve as additional or alternative indicators of distress. Accordingly, a list of tendons exhibiting exceptional tension conditions has been formulated.

Specialized procedures for vibration data acquisition were developed to permit characterization of an entire large bridge in a short time (days). Data processing and equation solution procedures tailored to this analysis were developed and implemented. A baseline of vibrational behavior for all tendons in the Niles Channel bridge was developed so that comparative measurements may be conducted over the remaining service life of the bridge. The results also revealed global trends of tension as a function of position in the bridge. For example, the tendons in the Atlantic side of the bridge were found to have typically lower tension (by about 5%) than those in the Gulf side.

Electrical testing consisted of measuring the electrical resistance of the tendon as a function of distance from the anchoring plate and determining whether the initial extrapolated value at zero distance and the slope conformed to those expected for an ideally sound tendon. This procedure is slower than the vibrational tests and has been conducted on a limited number of control tendons and others identified as suspects by the vibrational test. The preliminary tests showed a strong indication of distress by this method only in the one tendon known to have failed strands.

The procedures evaluated to date appear to be suitable for quick screening of the structure (vibrational) followed by more detailed analysis of suspects (electrical). Examination of the results available to date yielded consistent indications of distress only for the one tendon known to have failed strands. Electrical testing of the remaining suspects and periodic vibrational testing of the entire bridge is recommended.

Due to substantial evidence and previous history, it is recommended that all tendon segments adjacent to open expansion joints be subject to more intense scrutiny, including direct examination of the tendons.

Conditions leading to strand corrosion in the Niles Channel bridge need to be assessed, with special attention to the source and accumulation mechanisms of chloride ions, and to the factors that may affect corrosion performance after any remedial action is taken.

INTRODUCTION

Examination of post tensioned tendons of the Niles Channel Bridge during Spring, 1999 indicated severe corrosion damage and strand separation near the anchorage points on two tendons [1]. A second investigation was conducted on 7/14-15/99 to determine the suitability of mechanical and electrical testing of tendons [2]. Subsequently, an extended examination of all tendons in the bridge was begun in the period 8/16/99 to 8/20/99 [3] and a second phase was conducted during 10/26/99 to 10/28/99.

The goals of the extended investigation are as follows:

1. Develop techniques for measuring tension from dynamic response to excitation of the tendons and conduct these measurements

2. Develop methods for analysis of experimental measurements and apply these methods to the data obtained

3. Provide a baseline for all tendons so that comparative measurements may be conducted over the remaining service life of the bridge

4. Describe the tension of the tendons with respect to location in the bridge

5. Identify a candidate list of tendons exhibiting anomalous response that may indicate failed strands

6. Develop and implement an electrical resistance technique for further examining tendons from the candidate list for possible failed strands

The results of the first phase of the investigation have been detailed in the previous Reports [2,3]. The following sections describe the work conducted during the second phase and provide an updated description and interpretation of the overall findings.

WORK CONDUCTED DURING THE SECOND PHASE OF THE INVESTIGATION

The following tasks were accomplished during the October, 1999, a follow-up trip to the Niles Channel bridge:

1. A series of electrical resistance tests were conducted on a set of tendons identified as suspect as a result of the first survey.

2. A small number of tendons examined and analyzed during the first survey were found to be obstructed, so that they could not vibrate freely, resulting in uncertain data. These tendons were cleared of obstruction and retested in October. Data obtained were substituted for the original (flawed) data sets and reanalyzed.

3. The actual length of a small number of the tendons tested during the first survey was

found to be incorrect or in doubt. Measurements of actual lengths were substituted in the original data set and reanalyzed.

4. An experiment was conducted to assess the possibility of making static deflection measurements. Specifically, tendon 02MGT (see Nomenclature section) was deflected using a jack and lever arrangement, placed at the center. Deflection was measured by a dial gauge. An estimate of tension was made using elementary string formulas. The result of this measurement was a tension value of 141.3 kN/strand , compared to 119.5 kN/strand estimated previously [3]. No attempt to incorporate stiffness or boundary conditions into the measurement was made. Although the results were comparable with vibrational testing, the actual measurement procedure was quite difficult and would require considerable effort to adapt to some of the other tendons due to physical constraints. This method does not appear promising and is not recommended for future development.

5. Reproducibility and sensitivity checks were conducted for several tendons by placing the accelerometer in the usual position (see next section) but striking in different fashions, then moving the accelerometer to alternate positions and repeating.

6. The method of analysis of the data obtained was extended and refined.

VIBRATIONAL TESTING PROCEDURES

Data Acquisition And Initial Reduction

The method used for mechanical testing was the same throughout this investigation (given in the Interim Report [3]) and is repeated here for clarity. Mechanical testing consisted of manually hitting the tendons with a hammer, and recording the resulting vibrations for later analysis. A "dead-blow" hammer was used, hitting perpendicular to the tendon axis. The head of this type of hammer contains metallic shot in a yielding plastic enclosure, minimizing damage to the polyethylene tendon duct and reducing the chances for multiple bouncing impacts. Each tendon segment tested extended from the edge of the externally protruding portion of the metal duct nearest the end of the span, to the edge of the duct at the first deviation saddle from the span end (clear length denoted L). The impact point was at a distance ~1/6 L from the edge of the duct nearest the end of the span. The tendon was hit directly on the polyethylene duct, applying with the hammer an impulse as if driving a medium size nail. The hammer blow was typically in a near vertical direction. Hammer blows were applied after a delay of about 2 seconds and again after about 7 seconds from the start of the test. The second impact provided a repeat signal in case the first did not produce usable results. The total data recording interval was about 12 seconds.

A single axis accelerometer (Endevco 7703-50, SN KL61) was attached temporarily with wax to the polyethylene duct at a point distant ~1/3 L from the edge of the duct nearest the span end. The accelerometer axis was normally parallel to the direction of

the hammer blow, so that in-plane vibrational modes would be detected. Trial tests in the field indicated, however, that once excited the tendon vibration was not limited to a plane and usable signals could be obtained even in cases when the accelerometer axis was not parallel to the impact direction. The accelerometer was connected to an Endevco Model 2721B charge amplifier, and the output of the amplifier was connected to the line input of a laptop personal computer. Signal recording was performed using a Labview™ custom program acquiring stereo audio at an acquisition rate of 11,025 Hz and 16 bit resolution. Both channels recorded the same signal, but the Right channel had an external X ½ attenuator to act as a backup in case of signal overload of the Left channel (which was normally used for signal analysis). The impact strength was adjusted by the operator to minimize instances of signal overload. Later examination of the results showed satisfactory signal strengths and virtually no overload in all cases.

The Labview™ program created a *.wav file (typical size 0.6 MB) of the recording which was stored in the computer hard drive, and provided visual indication of the waveform and spectral distribution obtained, allowing for immediate feedback in case a test needed to be repeated. Figure 1 shows an example of the test response.

Initial data reduction was also the same throughout this investigation. After the data files were returned from the field, spectral analysis was conducted to determine the resonant frequency and overtones. This step was accomplished by means of a Fast Fourier Transform (FFT) analysis of the first 2^{16} readings (first ~6 seconds, which included the initial ~2 seconds of background signal plus ~4 seconds after the first blow) of the Left channel recording.

An initial program to compute the tension in the tendon (taking into account stiffness but assuming for simplicity a pinned condition at the tendon ends) from the spectra was developed. From these initial calculations a preliminary candidate list of suspect tendons was developed and submitted to the FDOT [3]. A more advanced approach, used in this report, is presented next.

Improved Analysis of Vibrational Response

After collection the response data were subjected to Fourier analysis as described previously [3]. The analysis returned a frequency spectrum for each tendon segment tested (see Figure 1). This information was in turn processed to determine the frequencies corresponding to the spectrum peaks so that a fundamental mode followed by a sequence of overtones was identified. This portion of the analysis was complicated by the fact that the overtones were not exact multiples of the fundamental, but rather were shifted slightly by the influence of the stiffness and end conditions (e.g. clamped or pinned) of the tendon [4,5]. Furthermore, it was noted that some tendons exhibited dual spectra (Figure 1), where individual overtones were found to be actually two peaks, with a slight frequency difference. Approximately one-third of all data have some separation of this nature. The existence of dual spectra and the slight frequency difference may be explained by a non circular arrangement for the strands within the tendon. Such a condition could develop as the strands are grouped as a flattened

rather than as a circular cross section. This core shape results from the strands pressing against the upper or lower side of the openings. At least two slightly different vibrational modes could develop as a result, and some degree of coupling between modes may exist.

In processing each spectrum, up to eight peaks were successively located with an automatic procedure by projecting ahead from the frequency of the previous peak. In some cases a peak would be poorly defined and the procedure could misidentify the location. Thus, a two-part test was implemented to select a final subset of peaks suitable for further analysis. First, only peaks having an amplitude twice the noise background were accepted, then the peak frequency sequence was fit to a polynomial and points deviating substantially from the smooth curve were automatically rejected. In this manner, it was found out that the fundamental frequency was usually poorly resolved compared to the overtones, and so was uniformly rejected.

To analyze the processed spectrum, the vibrating tendon segment was modeled as a dynamic system consisting of a flexible element under tension load and incorporating stiffness. The length of the segment was assumed to be equal to the distance between steel pipe rims at each end. In this improved analysis, the end constraints were treated as clamped. This assumption was made because the tendon is grouted into the pipe at either end, and the pipe itself is firmly embedded in either the bulkhead or the deviation saddle. The opposite extreme assumption would be to consider a pinned condition at each end. The pinned condition assumption (expected to be less accurate but easier to analyze) was used in the preliminary analysis described in September 1999 Report [3]. The material and geometric properties of the tendon (mass per unit length, elastic modulus, radius of gyration) can only be described as effective values due to the expected uneven distribution of grout and the unknown arrangement of strands inside the sheath. The tendon cross section was treated as a uniform material equivalent to the composite arrangement.

The system as described is governed by a fourth order differential equation [5]

$$T\frac{\partial^2 y}{\partial x^2} - QA\kappa^2\frac{\partial^4 y}{\partial x^4} = \rho A\frac{\partial^2 y}{\partial t^2} \qquad (1)$$

where y is the off-axis deflection, x is the length coordinate, t is time, and T is the tension. The variables Q, A, ρ and κ are the effective elastic modulus, cross sectional area, density and radius of gyration respectively (for the uniform equivalent tendon cross section). The tendon mass per unit length is the product $m=\rho A$, which can be calculated with reasonable accuracy from construction data on tendon dimensions and materials and thus used as a known parameter. The product $S=QA\kappa^2$ is called the effective stiffness, of which only rough estimates can be made without detailed knowledge of the geometry and elastic parameters and interfacial bonding conditions of the tendon cross section. Thus, S was treated as an unknown and solved for in the analysis of data.

As part of the present effort, an improved method for analyzing the observed spectra in the context of Eq. (1) has been developed. The input consisted of the tendon length, assumed end condition (clamped, for the present calculations), value of m, and frequencies of each of the peaks in the spectrum selected by the filtering procedure indicated above. Using the redundant, multiple peak information, both T and S were obtained as outputs of a numerical solution procedure. The procedure minimized a solution residual that served also as an indicator of the accuracy of the solution. If the spectrum contained dual peaks the spectra were assumed to reflect the superposition of two independent vibrational modes as indicated earlier. In those cases the procedure yielded two values of S, one for each of the modes, and a single value of T corresponding to the best compatibility with both modes. As expected, the peak series corresponding to the lowest frequency peak in each pair usually resulted in the lowest of the two S values obtained.

TENDON NOMENCLATURE AND INPUT PARAMETERS

The tendon and tendon segment designation is the same as used in the Interim Report. Each bridge span has six tendons, three in the northbound (Atlantic) side, and three in the southbound (Gulf) side. At each end of the span the tendons have slanting segments arranged so that one can identify a Top, a Middle and a Bottom tendon segment. The same tendon which is Top, Middle or Bottom at the Key West end of each span is also Top, Middle or Bottom respectively at the Miami end. Tendon segment designations in the following use a 5 character code exemplified by 17KGB: tendon segment located in Span 17, (K)ey West end of the span, (G)ulf side of the bridge, (B)ottom segment. The code 17GB without specifying K or M ends refers to the entire tendon. Unless specified otherwise, the term "expansion joint" will apply in the following to the four joints in main body of the bridge as well as to the two terminations of the bridge.

Table 1 shows the averages of actual length measurements (concrete-to-concrete distance) taken for each type of tendon end arrangement existing in the bridge. Within each type, variability in length was found to be small (typically less than 2.5 cm) except for expansion joints in the main body of the bridge, which showed ~10 cm variability. For force calculations, L was obtained by subtracting 10 cm from the amounts listed in Table 1, to account for the 5 cm of metal duct protruding from the concrete at each end.

For 19-strand and 27-strand tendons the values of the mass per unit length have been estimated from design data to be m=25.54 kg/m and m=29.80 kg/m respectively.

ELECTRIC RESISTANCE TESTS

Test principle

The electric resistance tests attempt to reveal strand breaks by the increase in resistance that would occur when one or more conducting paths are interrupted or degraded by breaks or loss of cross section. The principle of operation is shown in

Figure 2. A *dc* current I is made to circulate from a contact B made to the backside of the wedge plate to a remote connection B'. The potential difference P(x) between point C in the wedge plate, and point D located a distance x along the tendon from the wedge plate, is expected to be proportional to x if the tendon is sound and uniform. The corresponding resistance R(x) is defined as P(x)/I. Measurements of R(x) taken at tendon points accessible outside the trumpet area, and plotted as a function of x, should extrapolate to a resistance R(0)=0 . However if strands are broken, or if the cross section of the strands is smaller, inside the trumpet due to corrosion, the resistance R(0) should be a value >0 (i.e., a positive zero offset would be observed).

If strands were broken without substantial loss of cross section, the value of R(0) would depend both on the number of broken strands and also on the degree of lateral electrical continuity between strands away from the break. If the result of corrosion was simply the loss of cross section, R(0) would depend on the magnitude of the loss and the extent of this degradation along the strand. Since this information is not known beforehand, R(0) can only be viewed as a qualitative indicator of distress inside the trumpet, best suited for comparative evaluation of a suspect tendon against a population of reference tendons. Another indicator provided by the test is the slope given by $S_e = dR(x)/dx$. That value should equal ρ_e / A_c where ρ_e is the electric resistivity of the tendon steel and A_c is the sum of the total conductive cross sectional area of the tendon. For high strength carbon steel at room temperature $\rho_e \sim 0.2$ μΩ-m [6], while $A_c = 1.87\ 10^{-3}$ m^2 and $2.66\ 10^{-3}$ m^2 for 19- and 27-strand tendons respectively. Thus, values of $S_e \sim 11$ μΩ/m (2.8 μΩ/in) and ~ 75 μΩ/m (1.9 μΩ/in) respectively were expected in each case.

Test implementation

The test was implemented by establishing electric contacts (B' and B) for current insertion at the wedge plates of each end of the tendon to be tested, another electric contact (C) for potential measurement at the wedge plate of the tendon segment to be tested first, and four lateral contacts (D1 to D4) for potential measurements along that tendon segment. Contacts B, B' and C were made by drilling two 5/8" holes through the concrete pourback covering the wedge plate until it was exposed. Threaded rods with a sharpened end were then introduced through the holes and made to press against the back of the wedge plate by screwing through a metal tab fastened to the external concrete surface. Contacts D1 to D4 were made by drilling a 5/8" hole through the side of the tendon until exposing the side of a strand. A clamp with an adjustable, sharpened-end threaded rod was then fastened so that the sharp end firmly contacted the tendon. Contacts D1 to D4 were placed normally at 48" intervals starting at the point where the tendon exited the duct, closest to the trumpet. To evaluate the segment at the other end of the tendon, additional side contacts D'1 to D'4 (analogous to D1 to D4) and another wedge plate contact C' (analogous to C) were drilled there, using the existing contact B as the remote current contact and B' as the wedge plate current contact. Contact quality was verified by ensuring that mutual resistance was <1Ω between any two contacts in the tendon segment to be tested (the 4-point arrangement used eliminates errors from minor residual contact resistance).

Resistance measurements were made directly using a commercial *dc* bridge (AEMC Digital Micro-Ohmeter Model 5600) that drives a current of ~10 A through the current insertion points BB', automatically computes the ratio P/I for the potential measurement point chosen, and displays results with 1μΩ resolution. The measurements for each point were repeated with reverse current direction and averaged. In selected tendons the measurements were repeated once again using a new set of duct holes at the same x values but drilled 90° away from the first set.

The above describes the final testing protocol established; the position of the remote current insertion point and distance between potential readings varied somewhat when testing some of the initial tendon sets. The procedure in all cases was time consuming, typically requiring between one and three hours per tendon pair. The main delaying factor was establishing adequate side contacts along the duct. That step was made difficult by the small amount of metal (due to the surrounding grout) that is exposed at the bottom of the drilled hole. Alternative methods are being considered to effect contact rapidly while preserving the integrity of the strand.

RESULTS OF VIBRATION TESTING

Table 2 presents the tension results expressed as force per strand (T divided by the number of strands in the tendon) for each of the segments examined, analyzed by applying the clamped end assumption. Tables 3 and 4 show the corresponding values for the tendon stiffness S, from the low frequency and high frequency components of double peaks, respectively. If a test produced only single peaks, the same stiffness value was reported in both tables. Whenever multiple tests were performed in a given tendon segment, the results from the test yielding the lowest solution residual value were chosen for reporting. Sensitivity tests in which the accelerometer was placed in other positions yielded essentially the same results as those in the normal tests.

Figures 3 to 5 show the tension results by pairing each tendon segment tension with that of the mate (Key West-Miami ends of each bridge span). This pairing produces a data point in a graph formed by letting the X-axis represent the Key West end tension and the Y-axis the Miami end tension. A 45° line has been added to the graph for reference. Data for tendon segments with tensions identical with their mates would lie on this line. In Figures 6-9 the tensions are plotted as a function of bridge position. Figures 10-12 show the S values displayed in a manner similar to that used in Figures 1-3 for the tensions.

Several observations can be made from Figures 3-12:

1. Most tension values are below the nominal design value of 122,900 N per strand. The preliminary tension values reported in the September, 1999 Interim Report [3] were evaluated with a simplified model that considered only pinned conditions for the tendon segments. The present values (obtained with the advanced model that assumes a more realistic clamped end condition) are about 8% smaller than those estimated in the Interim Report. The present values are

believed to be a better estimate than before of the actual tendon forces because of (a) the more realistic end condition used (clamped); (b) the use of more accurate tendon length measurements, signal processing, vibration model, and method of equation solution; (c) fewer incidence of outliers in the population of results; (d) very few instances of results indicative of excessive tension (a condition that would have been generally avoided during construction). It is emphasized that even though the absolute values reported here are lower than previously estimated, the trends of the data and conclusions remain generally the same as before [3].

2. Most of the data in Figures 3-5 lie close to the 45° lines, so that both ends of each tendon have tensions that are typically within about 5% of each other. Thus, the combination of actual end-to-end tension variation (due to friction forces at the deviation saddles) and tension measurement uncertainty was usually relatively small. The locus of data is nevertheless biased in all graphs toward the region below the 45° line, suggesting that the tension in the Key West end of the tendons was on average about 2% greater than in the Miami end. The subset of tendons terminating at expansion joints was found upon closer examination to deviate somewhat from the overall bias. In these tendons the segment having the higher tension (by about 1.5% on average) was usually the one at the expansion joint, regardless of whether it was at the K or M end of the span. These biases may be the combined result of systematically tensioning the tendons from one end, followed by stress redistribution during settling (also reflecting different restraint conditions at the expansion joints).

3. The tension data (Figures 3-5) for the Atlantic side of the bridge cluster consistently around lower values than those for the Gulf side of the bridge. Figure 9 clearly shows that in the center spans of the bridge the Gulf side tension was about 5% greater than that of the Atlantic side.

4. Disregarding the expansion joint spans, within each side (Atlantic, Gulf) of the bridge, the average tension per strand (see Fig. 9) was typically greatest in the top tendon and smallest in the bottom tendon. These differences were small, typically on the order of 3%.

5. Figures 6-8 show that within each bridge side the tension per strand at the top tendon tended to be smaller at expansion joint segments (except for the end segments). This trend was either absent or much less pronounced for the middle and bottom tendons. However, in all cases tensions tended to be slightly smaller in the center spans of the bridge.

6. Tendon 19AM had tension values (~76 kN and ~72 kN at the K and M ends respectively) that were dramatically lower than any other in the bridge. The data for that tendon are indicated by arrows as being outside the range of Figures 4, 7 and 9. However, as indicated later, the electrical tests on this tendon did not reveal distinctive behavior. The tension results for 09AM, the only tendon

positively known to have failed strands, are identified in Figures 4 and 7 and discussed in more detail later.

7. Stiffness determinations are the result of minor deviations from harmonic behavior in the overtones. Scatter in the S values calculated from the spectra is expected to be due to a combination of variability in the stiffness property from tendon to tendon, and error in experimental determination. The results in Figures 10-12 show the S values obtained with the lower frequency peak set. The low frequency S values did not show any general bias toward either the Miami or Key West end of the bridge spans, or to the Atlantic or Gulf side of the bridge. This lack of bias is to be expected, as the stiffness should be mostly a function of the geometric arrangements of strands in the cross section of the tendon, and not vary significantly with location in the bridge. It is noted however that the high frequency S values showed some degree of bias for greater values on the Miami side, which has no apparent correlation at this time. The average of the 19-strand tendon S values observed (~1.25 10^5 N-m^2 for low frequency peak series, 1.4 10^5 N-m^2 for high frequency series) shows order-of-magnitude agreement with the value of ~1.2 10^5 N-m^2 estimated for an ideally bonded close-packed arrangement of strands and grout. As indicated earlier, a more accurate comparison with ideal behavior is not possible with the information available. The S values obtained for the 27-strand tendons (a small subset in Figure 10) were, as expected, higher than those for the 19-strand tendons. Again as expected, no separate trends could be identified for this group. As discussed later, neither tendon 09AM (failed strands) nor 19AM (very low tension) showed distinctive stiffness results.

IDENTIFICATION OF EXCEPTIONAL TENDONS FROM VIBRATION TESTING

Overall considerations

A principal benefit of the current study is the development of a baseline observation of tension for every tendon, using the vibrational testing technique. Comparison of results from each tendon segment from future inspections will provide one of the best means of detecting adverse changes that may have developed in the interim.

At this time, it is possible to identify specific tendons for subsequent detailed examination or more intense monitoring (a preliminary selection of tendons based on vibrational testing was reported in the Interim Report [3]; as a result several of those tendons were subsequently tested with the electrical method and the results are reported in the next section). It is emphasized that the identification of a specific tendon is only a statement of suspicious behavior. Likewise, tendons having flaws could escape detection using virtually any identification criterion. Most of this effort has been focused on examination of the vibrational testing data for evidence of failed strands. The following sections discuss possible indicators of tendon distress.

Possible indicator: Tension lower than peer group

It is expected that detensioning is one major result of strand breakage. As noted above, tension exhibited global variation along the bridge, from side to side, and from top to bottom within a given side. These global variations are assumed to reflect loading conditions not related to strand breaks. Under this assumption, simply looking for low tensions will not produce a good candidate list. Rather it is necessary to subdivide the tendons into peer groups, tendons of nearly the same length and location in the bridge, to define typical or average conditions for comparisons. Thus, to search for suspicious behavior each tendon tension was compared with the average of a peer group defined as follows.

The bridge was first divided into five sections, each between two expansion joints. Thus these sections , numbered 1 to 5, included spans 1-8, 9-16, 17-23, 24-31 and 32-39 respectively. Within each section the Gulf and Atlantic side were treated separately, and within each side the top, middle and bottom tendons were considered individually. This defined 30 separate tendon peer groups. For each peer group a restricted mean tension was computed using the results of both the Key West and Miami end tendon segments, but limiting the calculation to tendons not terminating at expansion joints. The tendons terminating at expansion joints were excluded (from the mean calculation) because those tendons often had extremal tension values (e.g., see Figure 6) which may reflect loading conditions different from those encountered elsewhere. A criterion for selection based on this indicator is given below.

Possible indicator: End-to-end tension difference

Detensioning due to strand breakage may also be detected by comparing each tendon segment tension to that of the segment at the other end of the tendon. To this end a tension difference ratio T_D was defined as the ratio of the difference in those tensions over the mean tension. Depending on whether the tendon was in a span adjacent to an expansion joint or not, T_D was defined as

$$T_D = \frac{T_O - T_I}{.5(T_O + T_I)} \qquad (2)$$

(span adjacent to an expansion joint)

$$T_D = \frac{T_K - T_M}{.5(T_K + T_M)} \qquad (3)$$

(span not adjacent to an expansion joint)

where T_O is the tension of the tendon segment immediately next to the expansion joint, and T_I the tension at the other end of the tendon. For spans not adjacent to an expansion joint, T_K and T_M are the tensions at the Key West and Miami ends of the tendon respectively. As indicated earlier, the tension results indicated that T_O and T_K were in most cases slightly higher than T_I and T_M respectively in each of the corresponding spans. Thus, T_D is in most cases positive as shown in Figures 13 and 14 for the cumulative distributions of T_D values per Equation (2) and Equation (3) respectively.

The median value of T_D in each case is about 0.02 (attributed to deviator friction), but some tendons have ratios as high as 0.06 while others actually have negative ratios. Such deviations may be revealing. If a strand in either end of a tendon were to break (with some resulting loss of tension), friction at the intervening deviator blocks would prevent complete transmission of that loss to the other end. This disparity would result in a value of T_D different from that prevalent in sound tendons. Thus, tendons with T_D values greatly different from the norm are potential suspects for failed strands. This possibility is strongly supported by the results for tendon 09AM, which is known to have failed strands in the segment 09KAM. As shown in Figure 14, 09AM has the most negative value of T_D in its category (tendons adjacent to expansion joints). Selection criteria based on the value of T_D are given below.

Possible indicator: Reduction in stiffness

Another result of strand breakage is expected to be a reduction in stiffness. The entire collection of tendon stiffness data appeared to be uncorrelated with other factors such as position, so simply looking for low stiffness tendons is reasonable. A selection criterion was formulated accordingly. It must be remembered however, that stiffness has only a second order effect in the analysis of the data and may not always be well determined. Thus some low stiffness values may represent measurement error only.

Special attention to tendon segments at expansion joints

The tendons terminating at the expansion joints represent a distinct group requiring special scrutiny. This group is exceptional in that the only tendon segment to have completely failed (09KGM) was at an expansion joint, as is the one still in place but with known failed strands (09KAM). The open expansion joints allow for direct exposure of the concrete pourback to the external environment, which is a possibly aggravating factor. Unusual loading at the expansion joint may have also been a contributing factor. The tension evaluations from vibration testing showed that the loading on these tendons is somewhat different that the majority of the tendons throughout the structure. Such condition is to be expected also from the different structural configuration at the joints, including the use of 27 strands vs the normal 19 at the top tendons. Because of these considerations, the spectral analysis of this group was performed both by automated and manual techniques for confirmation. The above indicates that this group of tendons (especially the segments immediately at the expansion joints) should be given priority in future examinations for signs of corrosion induced damage.

Criteria for selection

Based on the above, exceptional tendons were selected according to the following criteria:

1. Tension at either tendon end 5 % below restricted average (as defined above) in each group .

2. Tendons not adjacent to an expansion joint having the 5% lowest (2a) and 5% highest (2b) T_D values (all groups combined).

3. Tendons adjacent to an expansion joint having the 10% lowest (3a) and 10% highest (3b) T_D values (all groups combined).

4. Lowest 5% stiffnesses at either tendon end (all groups combined, but because of inherent difference in stiffness the 19-strand and the 27-strand tendon subsets were considered separately).

The 5% limit in Criterion (1) was chosen based on the 5% tolerance expected in posttensioning practice; greater deviations from the peer group average would then be considered suspect. The tendon fractions for the other Criteria were chosen to produce a manageably small number of tendons selected for further examination.

Table 5 is a tally of tendons satisfying any of the above criteria. Any tendon identified in more than one of those categories should be considered to be more strongly suspect and scheduled for additional testing. It is noted that the only tendon positively known to contain failed strands (09AM) met Criteria 1 and 3 (the latter by having the lowest T_D in its set). As indicated earlier, tendons such as 09AM and all others adjacent to expansion joints (zones highlighted in the Table) merit intense scrutiny in the future. Elsewhere, it should be noted that tendon 19AM had the lowest tension of any tendon in the bridge, and is considered exceptional irrespective of status against any of the other criteria.

It is emphasized that the identification of suspicious behavior is based exclusively on indications of detensioning obtained from vibrational testing, and that it is not possible (at this time) to isolate the effects of strand breakage from variations in loading in the bridge structure. Development of advanced vibrational approaches to resolve this issue [7,8] should continue.

As a result of the previous work in this project, some of the tendons in Table 5 had already been selected for further study and were subjected to electrical testing as discussed in the next section. Some other tendons not giving unusual tension indications were also tested electrically for comparison.

RESULTS OF ELECTRICAL TESTING

The tendons tested with the electrical method are identified by an (E) in Table 5. Figures 15 and 16 show examples of measurements of R(x) for Miami-Key West tendon pairs. Values of S_e and R(0) were obtained by linear regression that took into account all the resistance values obtained at each position. In Figure 15 the data from the 19MAM-19KAM pair yield nearly identical S_e values close to the ideal value of 2.75 μΩ/in expected, and values of R(0) that deviate from 0 by less than 30 μΩ. Figure 16 shows results from testing the pair 03MAM-03KAM. R(0) is, as in the case of the previous pair, very small. Both slopes (especially so that for 03KAM) are significantly smaller than in the case of 19MAM-19KAM.

Figure 17 shows a summary of all the results available to date, including the two values obtained in the July, 1999 visits for 08MGM and 09KAM during early method development tests (these two values must be considered as preliminary as no confirmation tests has been conducted using the regular test procedure). Excluding 09KAM, the tendons tested have $-50\ \mu\Omega < R(0) < 30\ \mu\Omega$, with an average value of -7.5 μΩ and a standard deviation of 24 μΩ. Those results suggest that in the group without 09KAM tendon-to-tendon variations (as well as the presence of negative values) stem primarily from uncertainty in the determination of R(0), which does not appear to deviate appreciable from 0. In contrast, tendon segment 09KAM has a value of $R(0) > 0$ by an amount that is several times the standard deviation of the rest of the tests. As 09KAM is the only tendon segment known to have failed strands in the trumpet, the results suggest that the electric test has the potential to detect strand distress (subject to future confirmation, especially for 08MGM and 09KAM). The electric test results for the other tendon segments do not provide any additional evidence of distress. It must be emphasized, however, that the absence of such an indication cannot guarantee that the tendon segment is sound.

The values of S_e were comparable to the ideal value (2.8 μΩ/in for 19 strands, 1.9 for 27 strands) for most of the segments tested. S_e was noticeably smaller than the ideal value for 03KAM and 15KGM. In those cases, it is possible that short circuits with adjacent tendons may have diverted part of the excitation current to parallel circuits, creating a measured value of S_e smaller than expected. Such deviation would have reduced proportionally the value of R(0), but not to an extent sufficient to mask a zero offset of the magnitude indicated by the preliminary test result of 09KAM. Nevertheless, it may be desirable in the future to represent the zero offset in terms of $R(0)/S_e$ as a means to avoid obscuring effects from current deviation.

Most of the tendons tested in this portion of the study were selected as a result of the preliminary examination of the bridge [3], but most also satisfied one (03AM, 04GT, 19AM) or two (08GM, 09AM, 13 AB, 15GM) of the criteria identifying exceptional behavior on the basis of the vibrational testing reported here (Table 5). For tendon 09AM both the electrical (preliminary) and vibrational test indications were consistent with each other and with the direct observation of strand breakage. Based on the electrical test results of the other tendons it is reasonable at this time to conclude that

strand breakage is less likely to be the cause of the exceptional tension indications in those tendons, and that their low tension (notably in 19AM) could have resulted from loading conditions instead. It is cautioned however that the development and application of electrical testing should continue and that these finding should be periodically reviewed in light of extended examination of the bridge.

DISCUSSION OF CORROSION ISSUES

The evidence uncovered during the June 1999 examination of tendon segment 09KGM [1] indicated that corrosion played a key role in the rupture. All 19 strands of the tendon showed signs of corrosion. It is likely that the first strands to fail were those that had suffered the highest cross section loss from corrosion. The stress on the remaining strands would become even greater than before if substantial strand-to-strand force transfer existed. Those remaining strands would fail afterwards either because of the resulting overload or in combination with further corrosion loss of cross section.

The June 1999 examination results also indicated that bleed water had accumulated at the upper portion of the failed tendon trumpet sometime in the past [1]. The remaining grout there had a substantial chloride content (2.3 pcy) which could have been responsible for corrosion initiation there even under highly alkaline conditions. After initiation, corrosion can become highly localized in a generally alkaline environment such as that created by the cementitious grout. Thus, local loss of wire cross section is not surprising.

The origin of the chloride inside the trumpet is not clear. The chloride contamination may have resulted from chloride rich water leaking down from the deck and into the pourback. Mortar extracted in June 1999 from a corner of the bulkhead of the opposite tendon in the Atlantic side (09KAM, which is known to have failed strands) did show a sizable chloride content (3.4 pcy). However, the pourback mortar outside the wedge plate in the fully failed tendon had a very low chloride content (0.05 pcy). An internal origin for the chlorides may merit consideration. Grout extracted (away from the trumpet) from the failed tendon and others in the bridge, had low to moderate chloride contents (0.6 to 0.1 pcy). If chlorides leach into the bleed water they could concentrate wherever bleed water accumulates, such as in the trumpet. As bleed water recedes or evaporates a higher chloride content than elsewhere would result. The possibility of corrosion development without external chloride contamination is supported by results from a 1993 investigation [9], which documented development of corrosion at the bleed water zone of laboratory tendon/grout assemblies made with several commercial grouts and admixtures. Thus, although tendons at expansion joints may be particularly vulnerable to corrosion, the risk for tendons at other locations should not be dismissed.

The results of the chloride analyses of grout and mortar performed during the June 1999 series have been documented [1]. Additional testing for possible chloride contamination should be conducted in samples from other tendons, especially those identified as suspect by the vibrational survey. In addition, it is important to ascertain the potential for chloride accumulation in bleed water for the type of grout used in the

Niles Channel tendons, and for any grout used for future repairs in the bridge. To this end, experiments similar to and improving upon those described in Ref [9] should be conducted with these materials.

The mechanism of corrosion initiation and propagation in the tendons and anchors is still largely unknown. Experiments should be conducted in test solutions replicating the bleed water composition and also under semi-moist conditions that may occur after the bleed water recedes or evaporates. Those tests would establish the maximum tolerable chloride contamination under those conditions [10,11] and relate it to the allowable chloride (or other contaminants) levels in the grout. The issue of how to handle the present inventory of tendons is critical. Tests should determine the potential beneficial/detrimental effects of filling any existing grout cavities, and the choice of filler materials which may include corrosion inhibitors.

CONCLUSIONS AND RECOMMENDATIONS

1. Vibrational testing of the entire Niles Channel Bridge was completed. As a result of this study a comprehensive data base of tendon tension derived from vibrational testing has been developed. Comparison with the results of future vibrational testing at regular intervals may a powerful method of detecting tendon deterioration.

2. A method used to recover tendon tension from the frequency response of the tendon was developed and improved in several ways. Several filters and checking steps were added to remove unreliable frequency information prior to analysis. It was concluded that the most reasonable assumption for the tendon ends was the clamped condition. Numerical analysis techniques were derived to permit recovery of apparent stiffness, in addition to tension.

3. Tension and stiffness characteristics possibly indicative of mechanical distress were considered, including low tension, low stiffness, and unusual tension disparity between both ends of a tendon. Tension disparity was extreme for 09AM, the one tendon known to have failed strands in the bridge. Tension was lowest by far for 19AM, a tendon that did not show unusual behavior upon electrical testing. A list of tendons exhibiting exceptional tension/stiffness conditions has been formulated based on these possible indicators (Table 5). However, it must be emphasized that these conditions could result either from strand breakage or structural loading.

4. A small group of tendons have actually been subjected to electrical testing, based on the result of preliminary vibrational testing. Those tendons appearing in Table 5 as having exceptional behavior and also having been tested electrically are noted. At present, it is reasonable to conclude that with the exception of 09AM these tendons are simply detensioned and do not show evidence of actual strand breakage. While the results of the electrical tests are as yet not totally conclusive, the method appears to be promising and is

recommended for future diagnostic work.

5. Due to substantial evidence and previous history, it is recommended that all tendon segments adjacent to open expansion joints be subject to more intense scrutiny. Such effort might include more frequent vibrational and electrical testing as well as studies of corrosion susceptibility (including pourback removal for visual inspection and chloride analysis).

6. Conditions leading to strand corrosion in the Niles Channel bridge need to be assessed, with special attention to the source and accumulation mechanisms of chloride ions, and to the factors that may affect corrosion performance after any remedial action is taken.

7. The vibrational method shows promise as a structural assessment tool. The tests revealed global tension patterns along and across the bridge. In particular, a trend of generally lower tensions on the Atlantic side of the bridge observed in preliminary work was confirmed. Further development and improved calibration of the vibrational tension estimation method is recommended.

REFERENCES

[1] R.G. Powers, "Corrosion Evaluation Of Post-Tensioned Tendons On The Niles Channel Bridge", FDOT Report, June 29, 1999.

[2] A. A. Sagüés, "Acoustic and Electrical Evaluation of Post-Tensioned Tendons of the Niles Channel Bridge. Preliminary Findings", memorandum to FDOT, July 17, 1999.

[3] A.A. Sagüés, S.C.Kranc, and R. Hoehne, "Development Of Methods For Assessing Condition Of Post-Tensioned Tendons Of Segmental Bridges", Interim Report to the Florida Department of Transportation Contract # BC374, 1999

[4] R. W. Young, "Frequencies of Simple Vibrators", p.3 -110, American Institute of Physics Handbook, McGraw-Hill, New York, 1962.

[5] P.M Morse, "Vibration and Sound", Mc.Graw Hill, N.Y., 1948.

[6] ASM Metals Handbook, 9th. Ed., ASM International, Metals Park, OH, 1978.

[7] A. Mehrabi and H. Tabatabai, J. Struct. Eng., Vol 124, p.1313, 1998.

[8] H. Zui, T. Shinke and Y. Namita, J. Struct. Eng., Vol 122, p.651, 1996.

[9] A. Ghorbanpoor and S. Madathanapalli, Report FHWA-RD-92-095, Federal Highway Administration, Pub. By Nat. Tech Inf. Serv., Springfield, VA, Dec. 1993.

[10] H.R. Hamilton, J.E. Breen and K.H. Frank, J. Bridge Eng., Vol.3, p.64, 1998.

[11] H.R. Hamilton, J.E. Breen and K.H. Frank, J. Bridge Eng., Vol.3, p.72, 1998.

Table 1. Tendon Segment Lengths (m) - Averages of Actual Field Measurements

Tendon	End Span, Miami End of Bridge		Normal Span		Span on Miami Side of Expansion Joint (except end spans)		Span on Key West Side of Exp. Joint (except end spans)		End Span, Key West End of Bridge	
	M	KW	M	KW	M	KW	M	KW	M	KW
Top	8.83 (1)	14.51 (1)	15.00 (4)	15.18 (4)	15.03 (7)	12.25 (7)	12.40 (7)	15.19 (7)	14.30 (1)	8.98 (1)
Mid	8.77 (2)	11.79 (2)	12.29 (5)	12.46 (5)	12.32 (8)	12.25 (8)	12.38 (8)	12.47 (8)	11.59 (2)	8.95 (2)
Bot	8.76 (3)	9.08 (3)	9.57 (6)	9.75 (6)	9.59 (9)	12.22 (9)	12.36 (9)	9.75 (9)	8.87 (3)	8.92 (3)

Notes:

a) M and KW indicate Miami or Key West end of span respectively.
b) Numbers in parentheses indicate tendon number per construction drawings
c) Differences M and KW ends reflect also presence of closure joint
d) Lengths are concrete-to-concrete. For tension analysis purposes, 10 cm is subtracted from listed length to account for protruding duct ends.
e) All tendons assumed to be 19-Strand except for (7) which are assumed to be 27-Strand

Table 2. Force per strand (Newtons)

	Key West						Miami						
	Top		Middle		Bottom		Top		Middle		Bottom		
	Gulf	Atlantic	Gulf	Atlantic	Gulf	Atlantic	Gulf	Atlantic	Gulf	Atlantic	Gulf	Atlantic	
END	119171	120737	118941	118112	117421	115763	122566	122632	114704	120737	121053	115921	END
2	119632	121842	118941	119263	116842	115118	114289	115211	114868	114868	110000	117368	2
3	122625	122118	122368	124145	116711	114750	118158	120461	119605	120395	116053	113224	3
4	124329	125066	121579	121684	120000	117237	117053	120921		116868	112697	113276	4
5	126447	122671	122171	119737	118026	113276	122763	121750	120921	118158	113816	107763	5
6	123776	123961	124408	118664	120000	118895	121474	122105	119737	116868	118684	114737	6
7	122632	122395	125434	120368	119868	121612	116039	118816	118289	113414	113487	110526	7
EX	109352	111296	121151	112079	118941	110467	111204	112500	117651	114105	117763	114566	EX
EX	113519	108889	118816	104737	119816	114658	112222	109259	119263	108947	117789	110921	EX
10	121013	117237	123553	114013	118618	111112	120000	116447	121474	112447	115132	107632	10
11	121197	113829	114750	115763	111645	105447	114013	112368	112079	110467	110513	102105	11
12	122579	114382	116684	105171	112368	103553	120276	110789	113368	103789	110697	99737	12
13	124737	118250	122901	112079	117632	99368	118526	114382	118711	108763	110882	95000	13
14	120737	114211	113000	107566	112079	104711	118987	111987	110921	104895	111618	103158	14
15	122671	110974	119263	108763	119342	110605	119355	110882	120921	105908	114842	108289	15
EX	114537	101019	120263	112724	114289	105263	114444	101574	121105	113947	114013	108026	EX
EX	99213	109537	119539	112539	115257	110421	97037	105926	116592	109868	115118	105395	EX
18	116132	110513	116868	111618	114105	105908	115118	109684	112816	108579	109868	103974	18
19	120921	111474	113461	75789	108763	104342	120092	109158	111158	71711	108487	104158	19
20	122632	111158	115526	111711	113737	111066	117697	109500	115026	109408	113684	107895	20
21	120276	114197	116039	109039	115211	110974	114382	110605	112908	106711	113276	110000	21
22	122947	115487	116684	111434	113829	109039	119632	112309	111020	109316	114842	107632	22
EX	103704	94815	119934	108164	115724	105724	100926	96806	120645	109316	117145	110789	EX
EX	113241	111620	119539	115671	121658	115118	112407	109537	115257	113829	120553	111711	EX
25	120046	114980	118987	108303	115072	112079	117697	111849	114520	103421	111895	110263	25
26	118342	112632	115763	108763	108303	102224	115303	110461	114658	107934	106579	104066	26
27	118250	109961	113158	106737	110467	104987	114750	107474	113184	104342	109474	102763	27
28	121934	115763	120737	115579	114704	110605	119474		116224	110145	111711	103605	28
29	121289	114105	117974	112724	118526	114197	123316	112862	116270	110053	113368	112303	29
30	116039	108026	115303	109500	109730	109224	113829	108579	110974	107612	105447	103553	30
EX	107222	105556	114842	112895	111342	108026	107870	105370	119632	113737	114980	110329	EX
EX	106481	104491	114013	114105	113921	107382	104815	106019	114842	113947	110789	105632	EX
33	119447	120461	119447	113921	115211	113230	118158	121776	115533	109500	110191	107382	33
34	122303	116776	115526	115533	114382	109868	119171	112862	113737	115809	111803	107658	34
35	121059	122211	115395	116362	108763	104480	117697	119171	112697	113553	107474	101763	35
36	119079	117789	115763	112447	109868	108395	117513	116224	115257	109342	108763	106184	36
37	120092	117651	119079	120276	118158	114342	116868	114934	115579	117632	111572	115809	37
38	121750	120000	120645	117237	115533	117329	120276	119579	117928	116961	112816	118289	38
END	119678	125434	119816	119079	114934	115763	123316	123408	121711	119217	118342	117237	END

Notes:

a) One row per bridge span. Span #1 is at Key West end of bridge.

b) First 6 data columns correspond to Key West end of span; last 6 to Miami end.

c) Top, Middle and Bottom tendon designations per Table 1. Gulf or Atlantic side as indicated.

d) No usable data available for 04MGM and 28MGT.

Table 3. Low Frequency Flexural Stiffness ($N\text{-}m^2$)

	Key West						Miami						
	Top		Middle		Bottom		Top		Middle		Bottom		
	Gulf	Atlantic	Gulf	Atlantic	Gulf	Atlantic	Gulf	Atlantic	Gulf	Atlantic	Gulf	Atlantic	
END	136021	121630	104964	120185	165993	140063	125586	132241	132582	118704	118871	123647	END
2	117062	113762	114553	119274	110476	128741	167285	112619	119583	108777	125394	111843	2
3	125662	130093	109418	121669	109518	119315	138214	125820	114309	104771	122738	106756	3
4	114676	121359	113366	115524	107807	120735	118180	115749		114099	134646	119922	4
5	112395	116905	102530	114589	110992	128331	131282	126250	124647	125735	107191	120528	5
6	115165	129155	113896	118922	107992	115817	131290	122909	120535	114737	119393	110267	6
7	127285	118033	121875	124800	116337	124166	126924	114107	119498	120238	106977	120895	7
EX	209106	200964	103501	125458	126773	120683	219435	241740	144587	137472	146950	166594	EX
EX	201868	199142	160966	145955	146676	139218	198082	223599	152181	126457	115719	111758	EX
10	128344	120202	102370	136524	116381	119616	125372	114519	123247	125920	121424	122008	10
11	123703	129084	141646	127573	116130	116320	144917	121495	141807	137260	130849	114366	11
12	121322	118730	113158	124949	117048	122568	114426	131799	139295	124722	115502	112904	12
13	122603	117316	118563	135502	103914	108200	121684	135859	113985	128282	129862	107605	13
14	129757	124683	112555	120971	119107	125871	135442	141910	158437	122705	120548	116364	14
15	123992	126605	104469	134576	105901	124805	114761	127606	124647	116869	114661	110171	15
EX	198408	181520	110837	125023	130277	123604	204804	214305	130898	153599	190131	125220	EX
EX	201526	200160	146935	125019	166780	138097	222337	215212	129156	126084	116543	120197	EX
18	116382	137020	119510	129696	122452	115050	131637	120129	151953	131469	123991	119822	18
19	126261	109200	113018	132359	125146	119857	129410	143221	137802	143507	120570	116317	19
20	110825	131699	130876	139986	104676	125484	128715	121767	123540	141132	111999	117628	20
21	125433	124371	122180	127077	112428	131375	138832	125451	125772	123792	108037	120111	21
22	123906	128280	125716	123155	123266	125420	127246	136808	121000	121408	129692	120401	22
EX	196796	189645	103492	127750	116083	127331	204655	205808	126647	137402	154372	117763	EX
EX	207531	180195	128441	132034	136795	111534	207668	179104	126447	124295	124922	111430	EX
25	118832	116545	124912	121433	121050	116588	113141	144104	126224	118133	120398	112051	25
26	119077	129664	128736	127996	119880	125761	124279	136754	135482	122681	136758	126829	26
27	132663	129307	129303	132970	123515	120210	128427	145791	130583	134746	113759	105075	27
28	136266	122245	121131	121385	127682	127744	112669		162372	134045	129763	120849	28
29	118130	123620	118929	121984	119577	123735	123717	125186	131050	126057	113291	129772	29
30	145749	124048	139220	136834	129791	138154	149925	123783	132593	125112	128313	119629	30
EX	211839	206990	127897	125577	129485	115835	227196	202723	138778	130158	172784	175277	EX
EX	191324	198114	143246	126560	138474	137279	227398	221981	144080	109802	136957	119809	EX
33	126010	125469	118806	126051	125649	121785	123656	124261	127972	139619	127702	123347	33
34	128021	135126	129814	126800	119725	116431	116494	126312	147374	126185	123067	115762	34
35	123706	122702	115794	116121	118227	124495	120859	117570	124256	119277	130102	117835	35
36	137600	125725	122431	124529	113150	120777	138753	136918	135516	121050	104904	123736	36
37	141887	130806	131092	124759	133827	122890	130149	136385	138149	125370	131235	124144	37
38	126273	127256	123552	134090	122895	127499	120733	119749	134189	115164	128639	112306	38
END	119397	122299	115564	125864	109703	122074	119147	129796	115240	138028	132413	133543	END

Notes:

a) One row per bridge span. Span #1 is at Key West end of bridge.

b) First 6 data columns correspond to Key West end of span; last 6 to Miami end.

c) Top, Middle and Bottom tendon designations per Table 1. Gulf or Atlantic side as indicated.

d) No usable data available for 04MGM and 28MGT.

Table 4. High Frequency Flexural Stiffness ($N\text{-}m^2$)

	Key West						Miami						
	Top		Middle		Bottom		Top		Middle		Bottom		
	Gulf	Atlantic	Gulf	Atlantic	Gulf	Atlantic	Gulf	Atlantic	Gulf	Atlantic	Gulf	Atlantic	
END	136021	121630	124021	136213	159771	140125	152449	132241	147537	145548	153736	169621	END
2	124153	139545	137581	149520	75302	140073	161838	217955	158561	178664	125394	166068	2
3	170630	130093	146973	121669	134243	119315	207101	134175	163912	184468	112236	194365	3
4	114676	121359	167405	134324	164452	123641	199711	190929		131937	146470	139117	4
5	147630	116905	167568	162169	166019	135339	123741	126250	124647	125735	69034	164573	5
6	162113	129155	149281	141930	133021	124305	203670	122909	158177	162290	119393	151477	6
7	127285	118033	125312	124800	116337	123985	126924	168285	170619	159191	239066	174248	7
EX	235574	200964	133571	135646	125435	130064	240331	241740	146501	195964	181844	168381	EX
EX	220836	199142	197331	145955	147838	141610	241197	248491	177448	163021	115392	184765	EX
10	128344	120202	144220	136524	152196	126874	171610	169161	114225	128374	152467	136634	10
11	123703	129084	155269	126295	138457	123260	172020	172255	170910	159504	162635	175028	11
12	121322	118730	113158	124949	117048	122568	114426	131799	185001	175420	115502	112904	12
13	122603	117387	114821	134197	103914	108200	121684	176388	113985	193451	129862	107605	13
14	129757	124683	107774	114581	117224	137389	135442	171628	158437	153670	120548	116364	14
15	123992	126605	105685	134576	105901	124989	114761	127606	124647	114367	114661	110171	15
EX	198408	181520	149926	125023	156823	126950	253245	239964	130898	153599	190131	181849	EX
EX	215683	200160	146935	125019	162413	139992	222337	277559	129156	174499	116543	130315	EX
18	154143	146009	119092	129696	119272	123977	131637	130594	151953	164413	123467	119822	18
19	126261	184584	113018	132359	124407	120540	129410	143221	135044	143507	120570	118584	19
20	110825	131699	130876	139986	104676	125831	128715	121767	124788	166697	173866	175564	20
21	125433	124371	122180	133392	112428	131375	138832	125451	125772	123792	108037	186321	21
22	123906	128280	125652	124009	120835	135757	127246	153946	206145	170429	129692	120401	22
EX	242612	189645	163909	123099	130239	125658	204655	226045	136757	137402	152641	117763	EX
EX	207531	212580	128441	145599	138066	136294	207668	271211	153455	158432	121644	111430	EX
25	151755	127792	124912	121433	138956	116588	113141	135507	144601	165595	136942	204079	25
26	119077	142169	128736	127996	119124	125761	124279	146465	142897	122681	153772	129884	26
27	122322	141787	130922	129597	116663	120210	128427	135910	143095	131297	113759	105075	27
28	122613	115500	119351	121336	133350	139148	180675		162372	163353	149407	120849	28
29	148081	160425	118929	141826	116650	123678	123717	184888	146885	173035	113291	139879	29
30	145749	149080	133233	136834	133062	138154	149925	168689	132593	153262	128313	152146	30
EX	211839	206990	139452	125577	127221	131401	227196	242452	138778	186112	161057	175277	EX
EX	204478	208581	139290	126401	138474	137279	227398	221981	145337	177826	144701	118462	EX
33	126010	132288	118806	126051	125649	137336	118324	142888	129857	187577	136794	123347	33
34	124614	135126	129814	140303	119725	116431	116494	166151	147374	151688	123067	115762	34
35	128831	122702	115531	156896	125777	134417	120859	126871	126479	179675	130770	117835	35
36	164857	152447	153526	124529	113150	137703	129104	164390	145119	198380	104904	177010	36
37	141887	161132	131092	125876	135398	122890	130149	157374	138149	182551	131362	120272	37
38	126273	129617	123552	138319	124851	124891	120733	148658	145653	119866	149144	112306	38
END	142230	122299	180342	125864	109537	133868	119815	129796	179752	138307	131090	150803	END

Notes:

a) One row per bridge span. Span #1 is at Key West end of bridge.

b) First 6 data columns correspond to Key West end of span; last 6 to Miami end.

c) Top, Middle and Bottom tendon designations per Table 1. Gulf or Atlantic side as indicated.

d) No usable data available for 04MGM and 28MGT.

Table 5. Tendons exhibiting unusual behavior according to Criteria 1-4 in text.

Span	TOP		MIDDLE		BOTTOM	
	GULF	ATLANTIC	GULF	ATLANTIC	GULF	ATLANTIC
1	3a		3b 4	3a	3a	
2	1	1		4	1 2b	2a
3			4	4 E	4	4
4	2b E		*		2b 4	
5			4		4	
6					4	
7			2b	2b	4	2b
8			3a 4 E			3b
9				1 3a † E		
10			4			
11	1 2b					
12						
13					2b 4	1 4 E
14			1			
15			2a 4 E		4	
16	E	1 4				1
17	1	1 3b				1 3b
18						
19		4	E	1†† E		
20					4	
21					4	
22					2a	
23	1 3a	1	4			1 3b
24		4	3b			
25						
26						2a
27						4
28		*				2b
29	2a					
30		2a			1	
31	1	1	3b			
32	1	1				1
33		2a				
34						
35						1
36					4	
37						2a
38						2a
39					4	

*: Incomplete data †:Failed strands ††:Markedly low tension
E: Tendons tested electrically

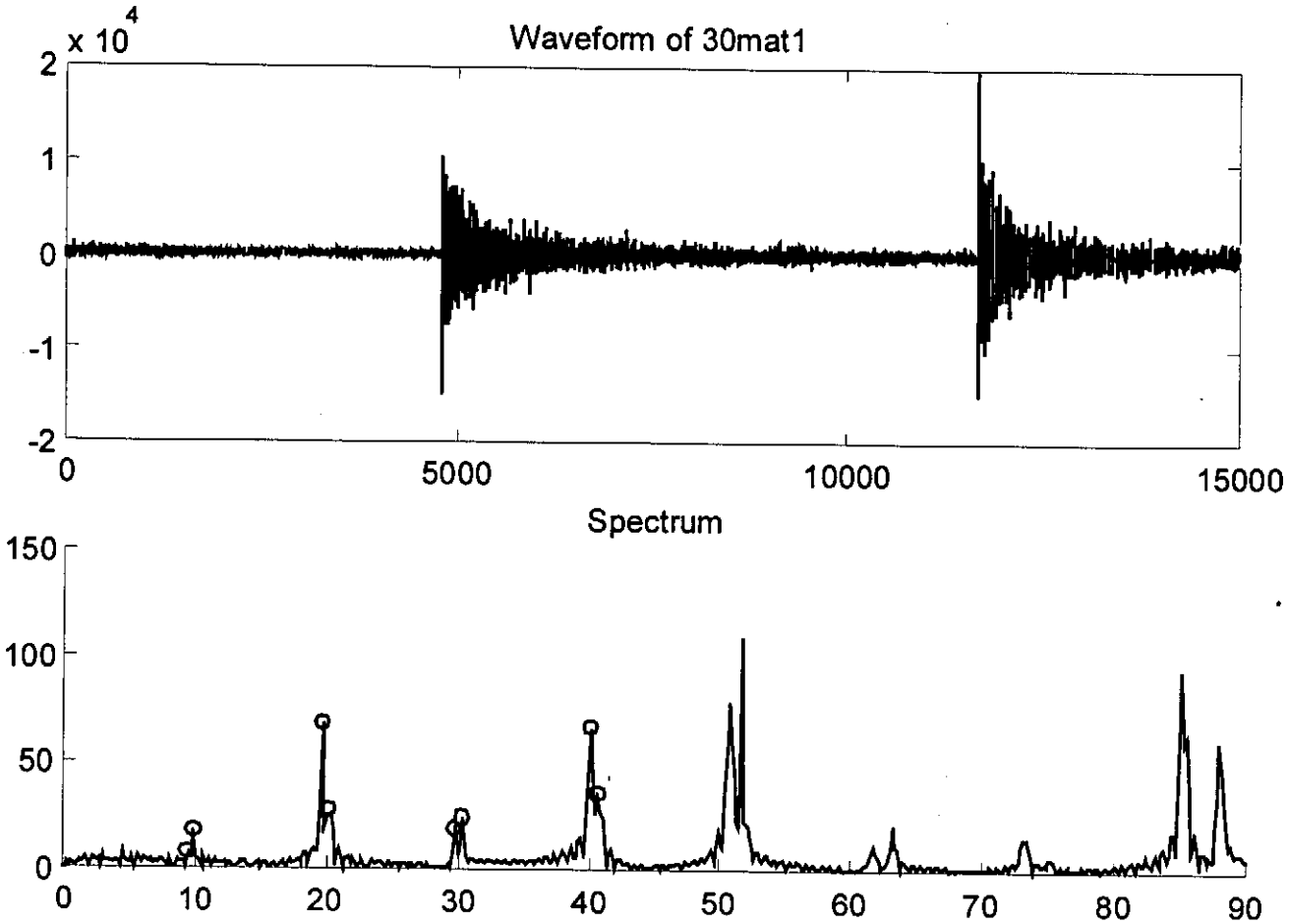

Figure 1. Example of waveform data and spectral analysis for a typical case (tendon segment 30MAT). The waveform contains 150,000 data readings (plot scale is 1/10). In this example the period before the first hammer hit was about 4 seconds. The vertical scale is in arbitrary units in both graphs. The spectrum horizontal axis is in Hz. Notice the closely spaced dual peaks.

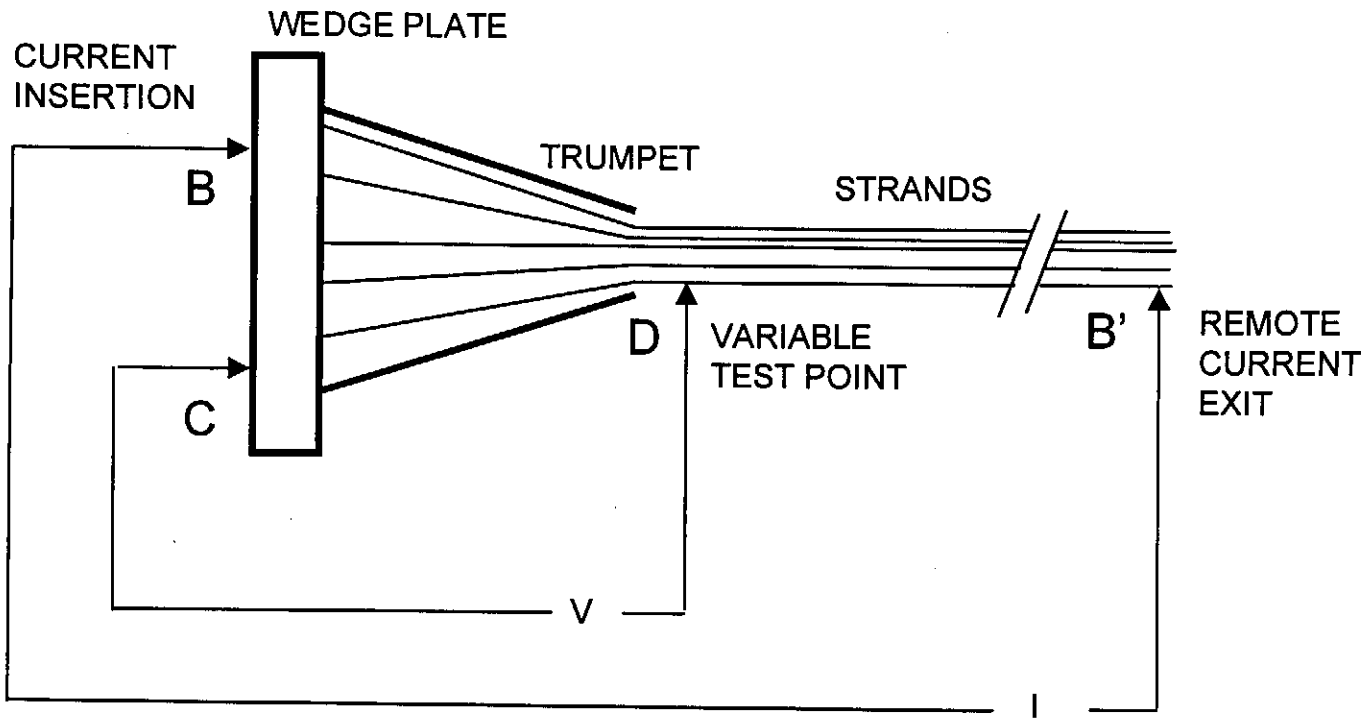

Figure 2. Schematic of electric resistance test.

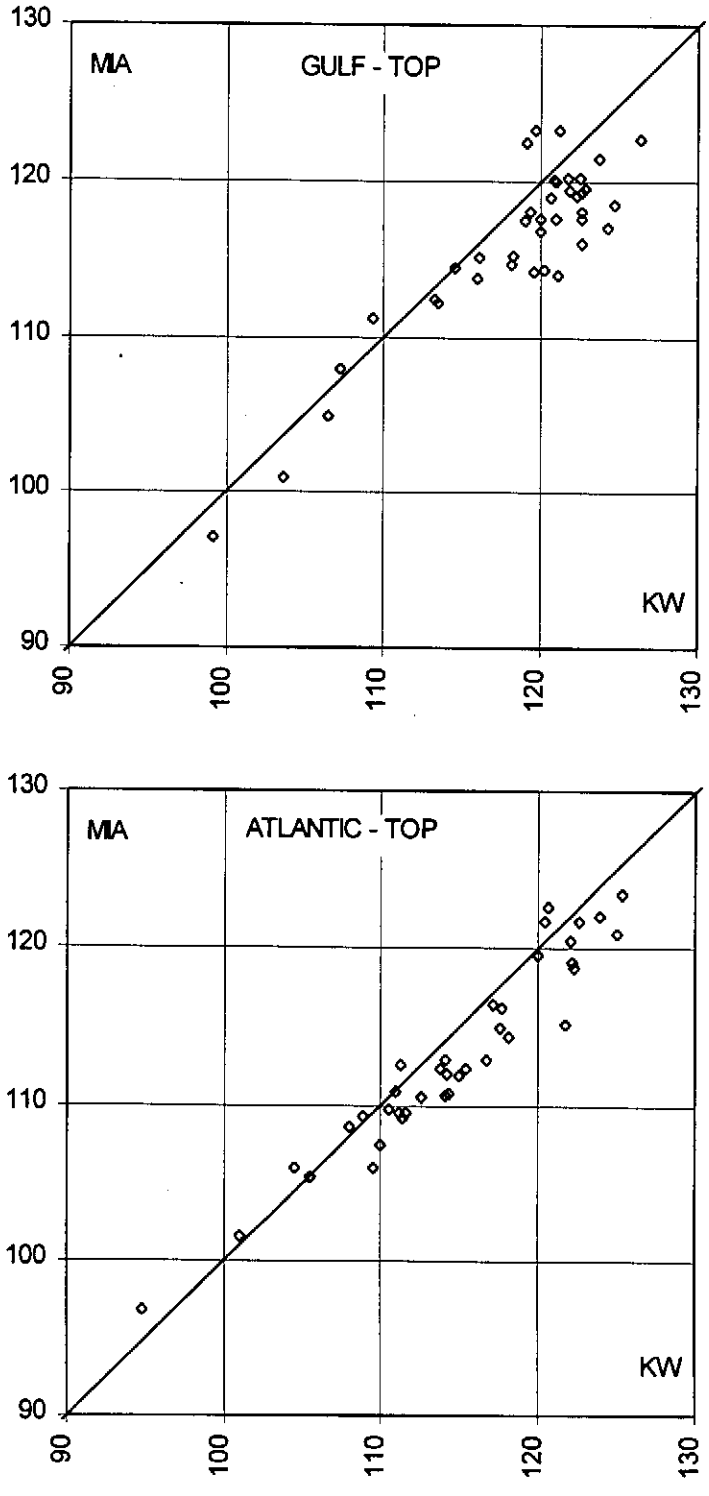

Figure 3.Calculated force per strand (kN) at the Miami end (MIA), as function of the force at the Key West end (KW), of each Top tendon in the bridge. An ideal 1:1 diagonal line is shown for reference. The upper and lower graphs are for Top tendons on the Gulf and Atlantic sides of the bridge respectively.

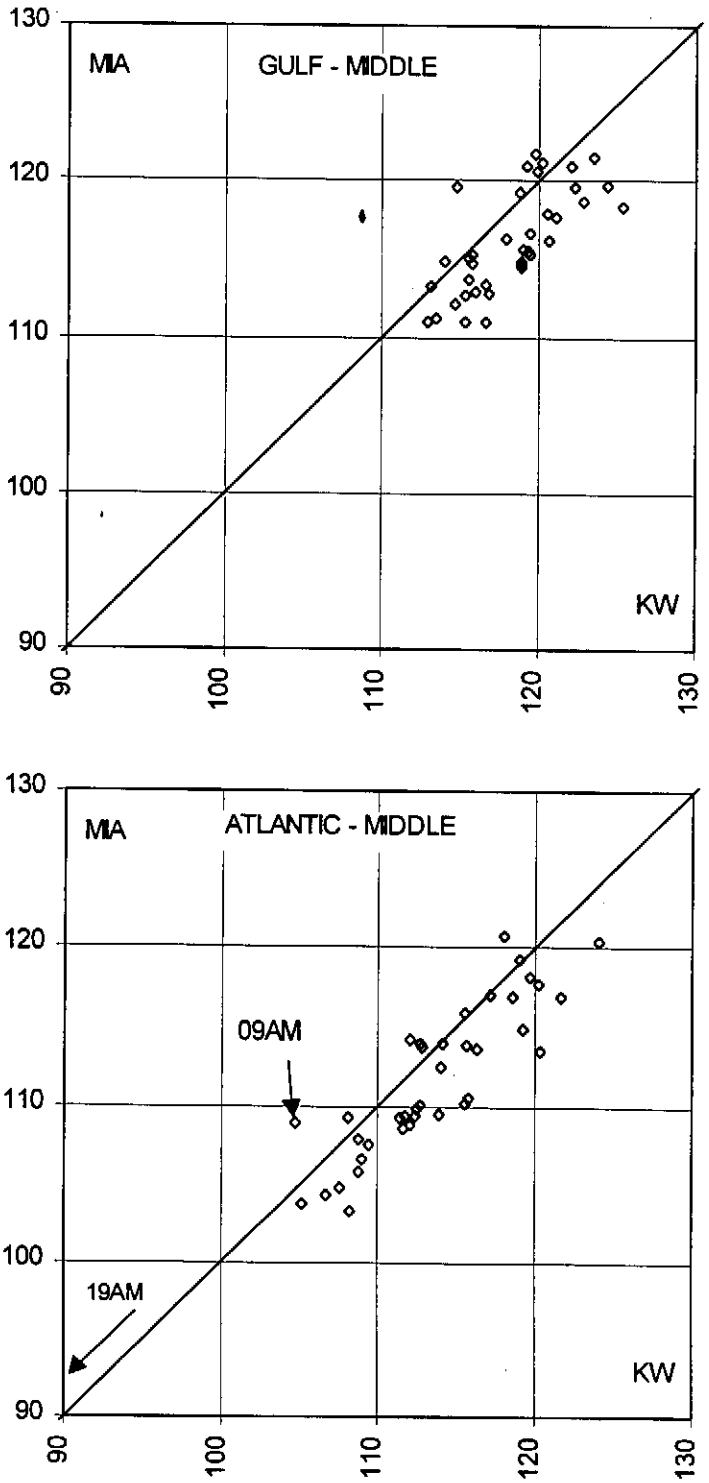

Figure 4. Calculated force per strand (kN) at the Miami end (MIA), as function of the force at the Key West end (KW), of each Middle tendon in the bridge. An ideal 1:1 diagonal line is shown for reference. The upper and lower graphs are for Middle tendons on the Gulf and Atlantic sides of the bridge respectively.

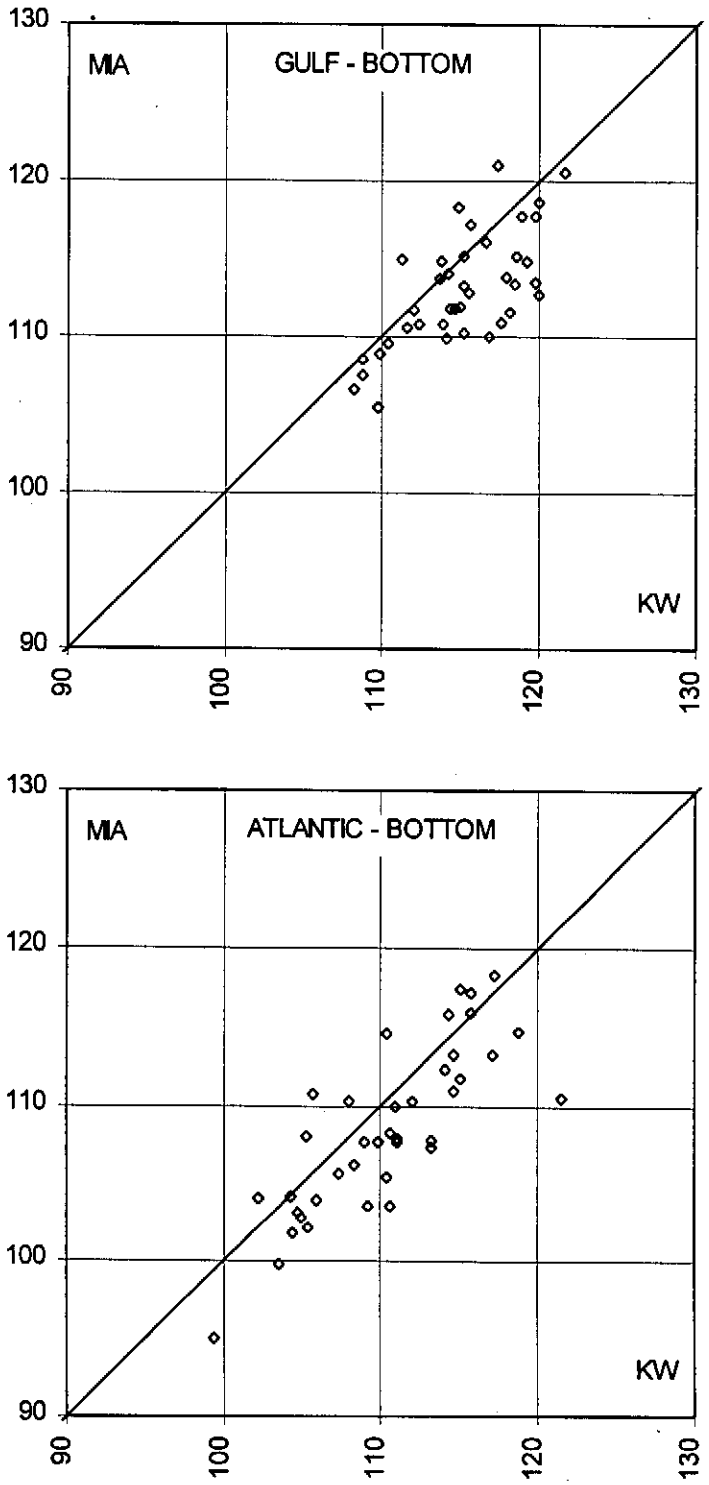

Figure 5. Calculated force per strand (kN) at the Miami end (MIA), as function of the force at the Key West end (KW), of each Bottom tendon in the bridge. An ideal 1:1 diagonal line is shown for reference. The upper and lower graphs are for Bottom tendons on the Gulf and Atlantic sides of the bridge respectively.

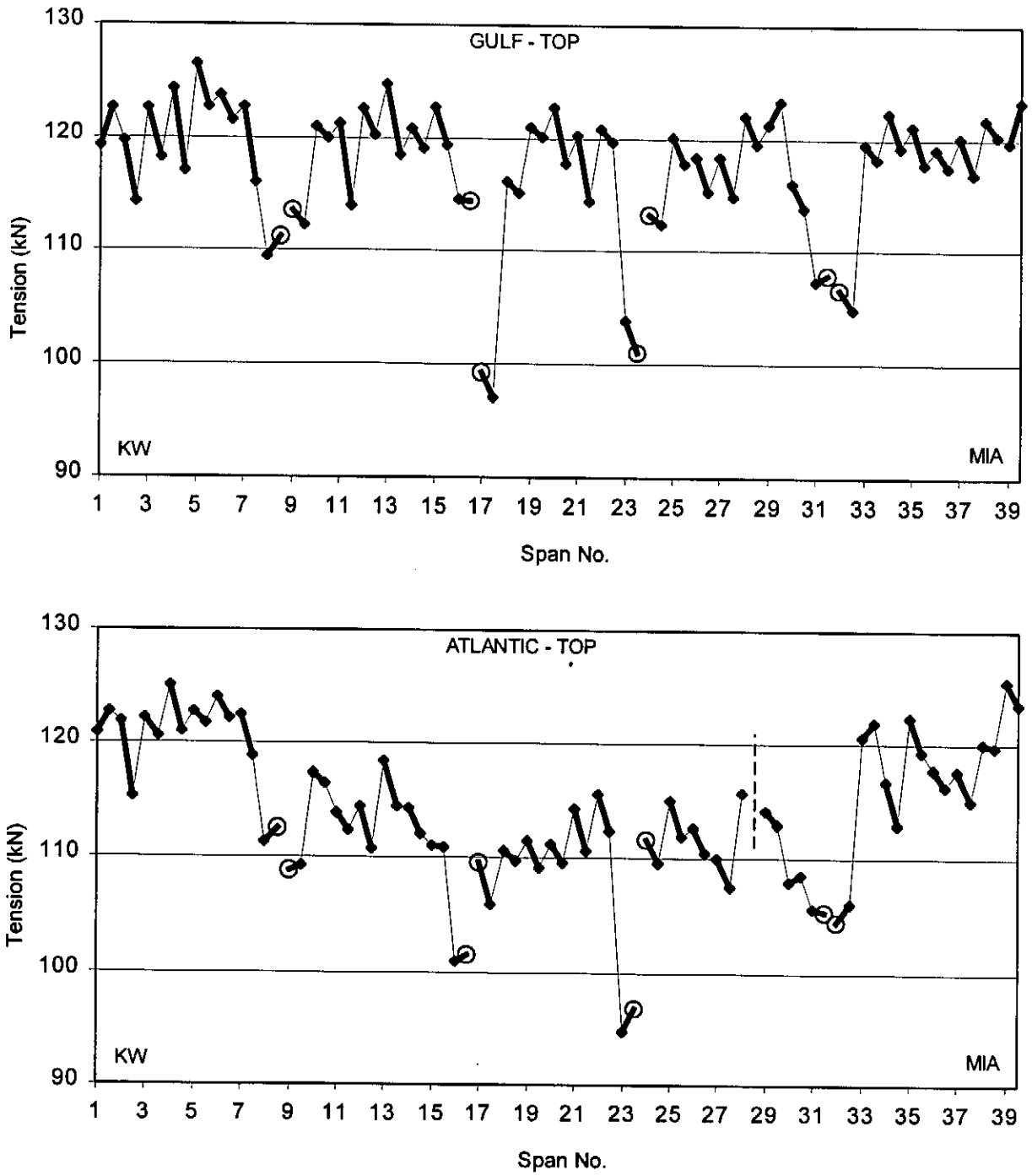

Figure 6. Tendon segment tension (force over nominal number of strands) plotted as a function of position along the bridge for Top tendons, Gulf and Atlantic side. The heavy lines join the symbols for Key West end (left) and Miami end (right) of each tendon. Larger circles indicate tendon segments terminating at expansion joints (gaps in line other than bridge ends). Vertical dashed line denotes data not available .

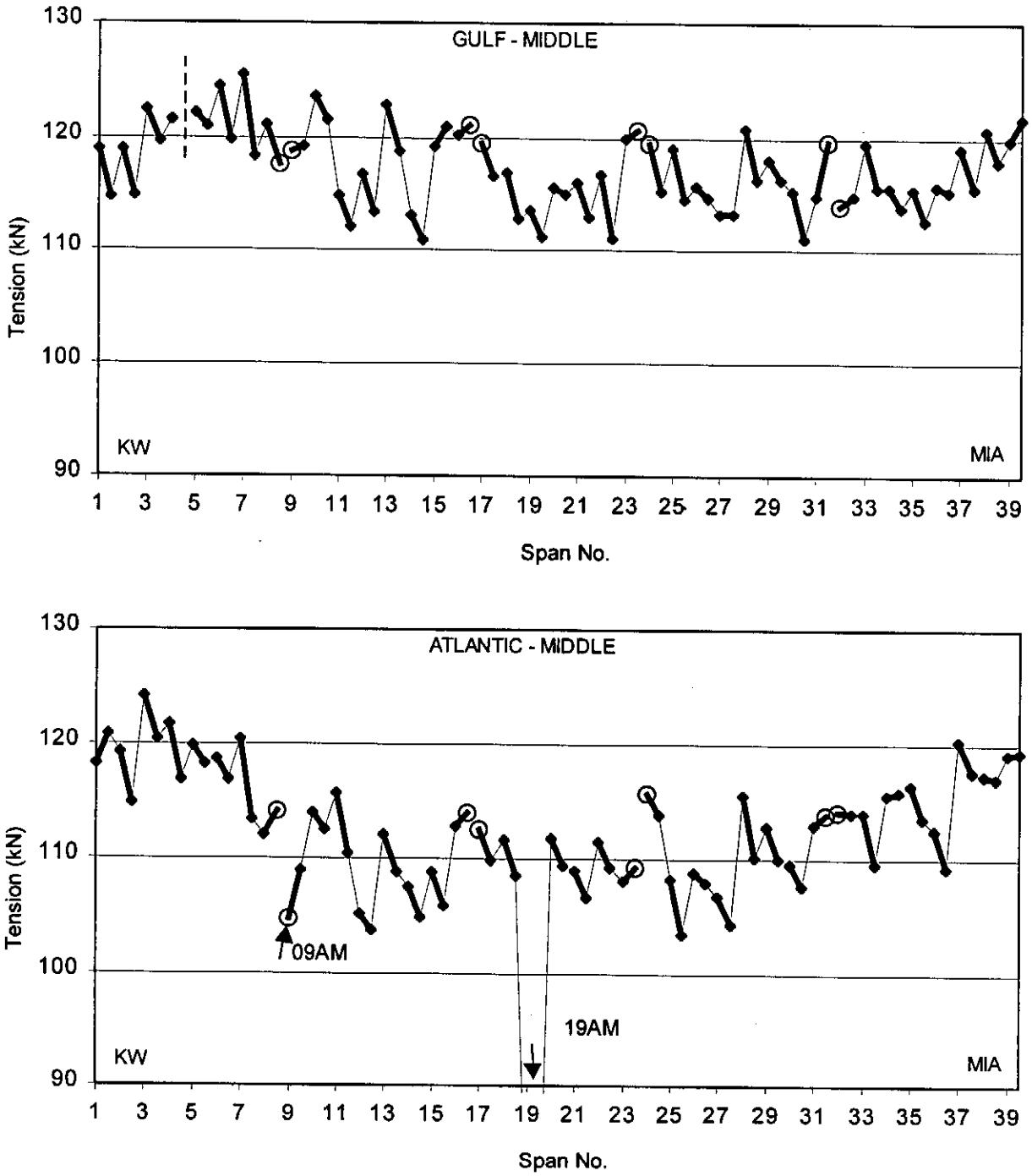

Figure 7. Tendon segment tension (force over nominal number of strands) plotted as a function of position along the bridge for Middle tendons, Gulf and Atlantic side. The heavy lines join the symbols for Key West end (left) and Miami end (right) of each tendon. Larger circles indicate tendon segments terminating at expansion joints (gaps in line other than bridge ends). Vertical dashed lines denote data not available.

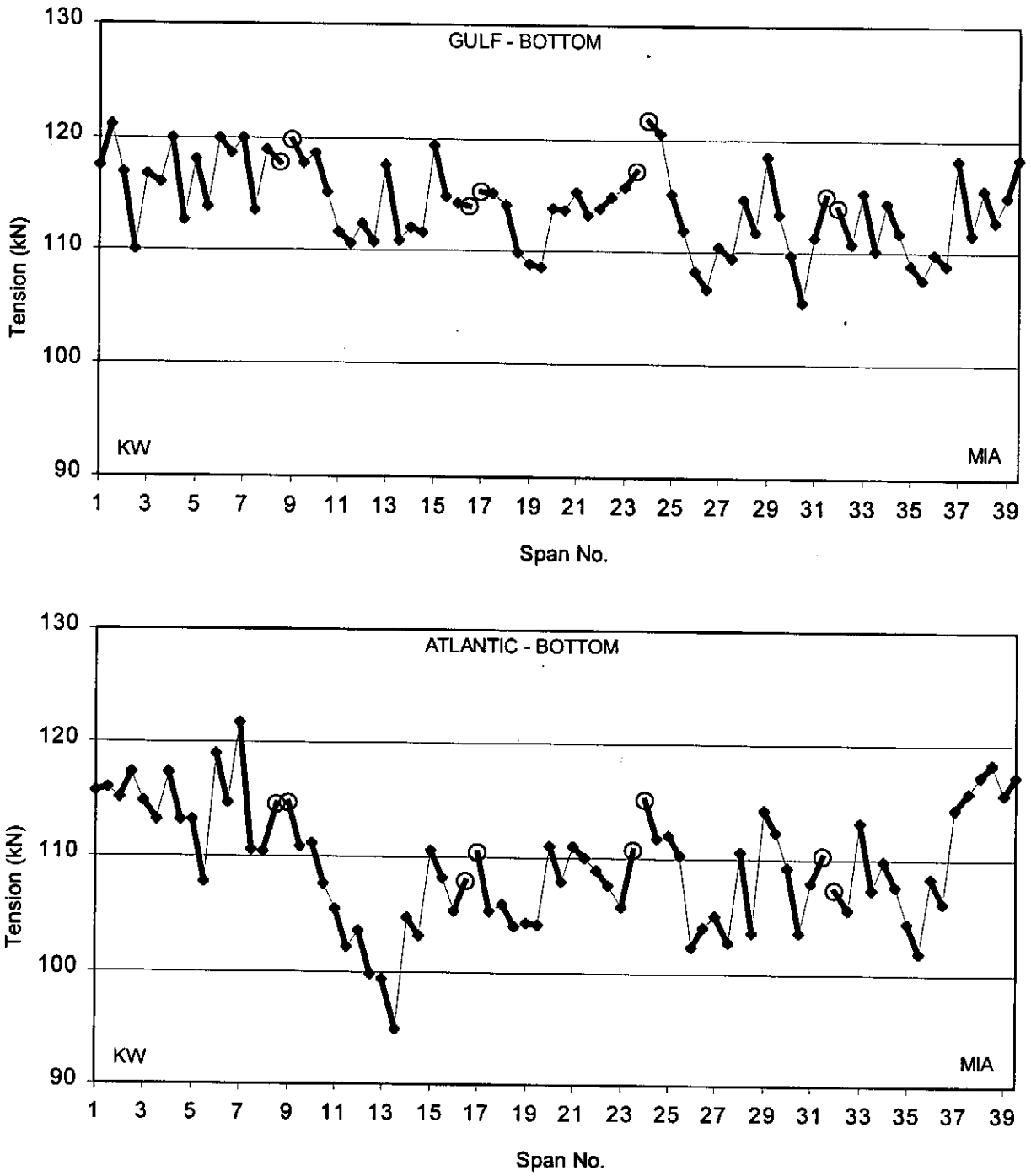

Figure 8. Tendon segment tension (force over nominal number of strands) plotted as a function of position along the bridge for Bottom tendons, Gulf and Atlantic side. The heavy lines join the symbols for the Key West end (left) and Miami end (right) of each tendon. Larger circles indicate tendon segments terminating at expansion joints (gaps in line other than bridge ends).

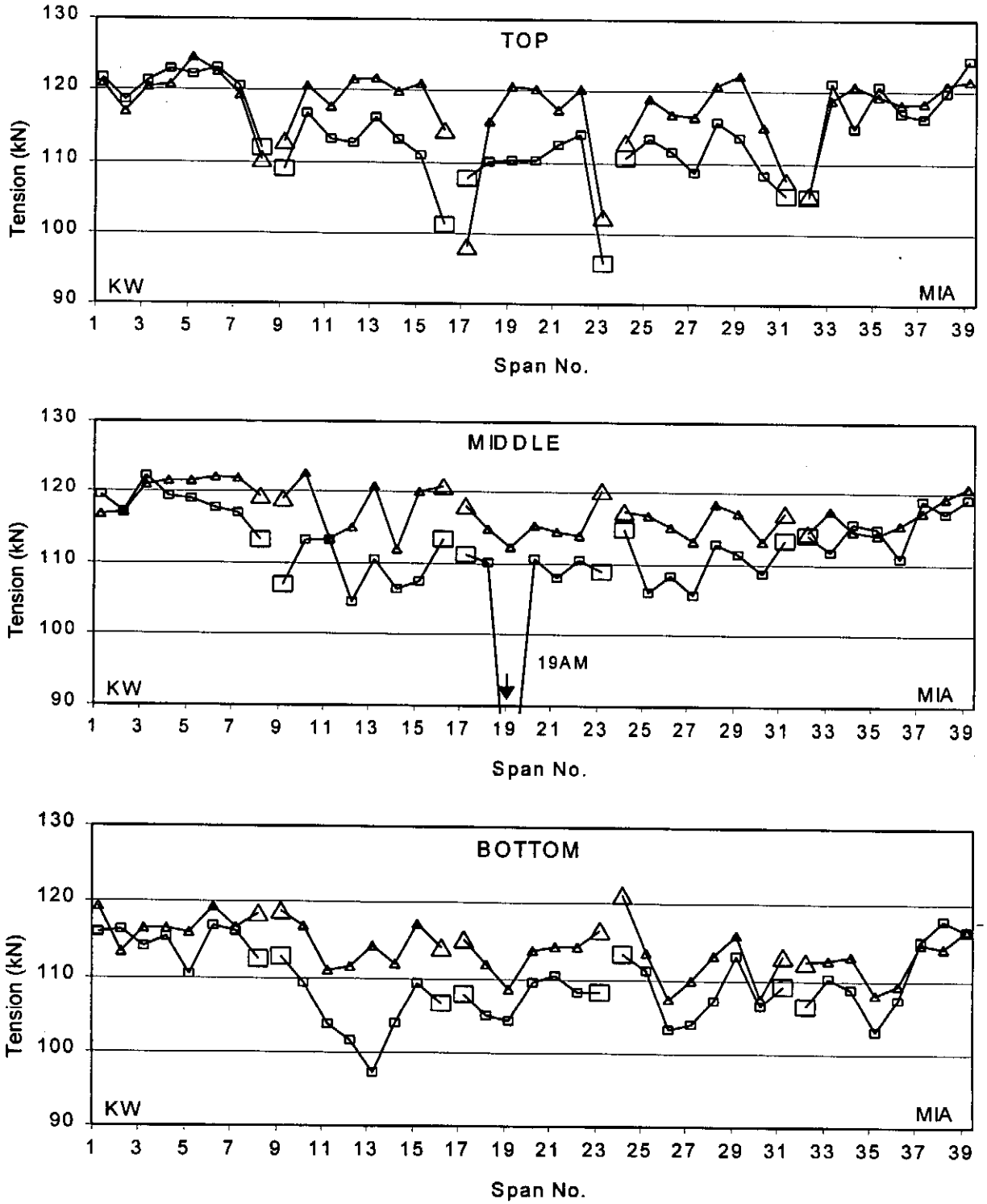

Figure 9. Average tension (force over nominal number of strands) of tendons on Gulf and Atlantic sides along the bridge. The Key West end is at Span 1. Larger symbols indicate tendon segments terminating at expansion joints (gaps in line other than bridge ends). Note general lower tension in Atlantic side (box symbols) than in Gulf side (triangle symbols).

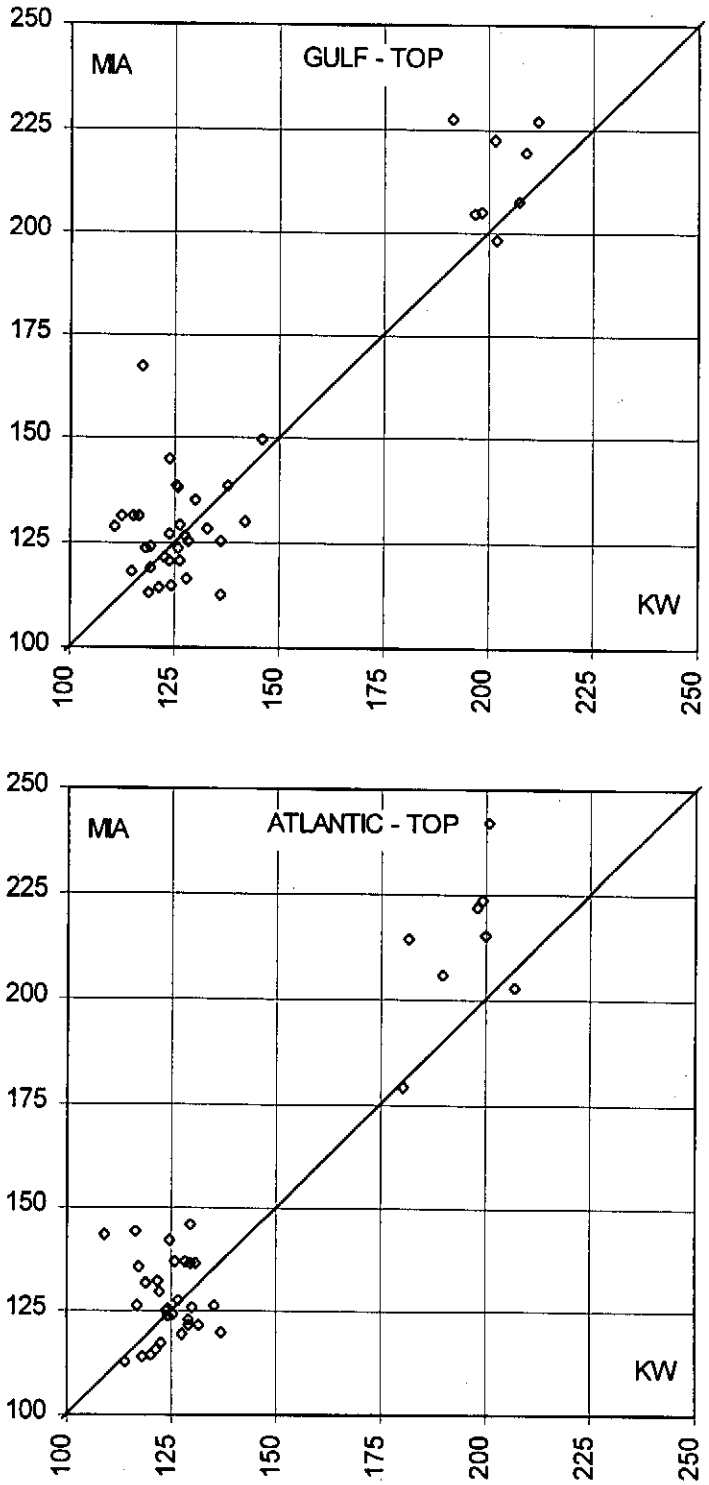

Figure 10. Calculated stiffness (kN-m^2) at the Miami end (MIA), as function of the stiffness as the Key West end (KW), of each Top tendon in the bridge. An ideal 1:1 diagonal line is shown for reference. The upper and lower graphs are for Top tendons on the Gulf and Atlantic sides of the bridge respectively. The group of 8 symbols with higher stiffness values corresponds to the 27-strand tendons. The results shown are obtained using only the low frequency component of the double peaks.

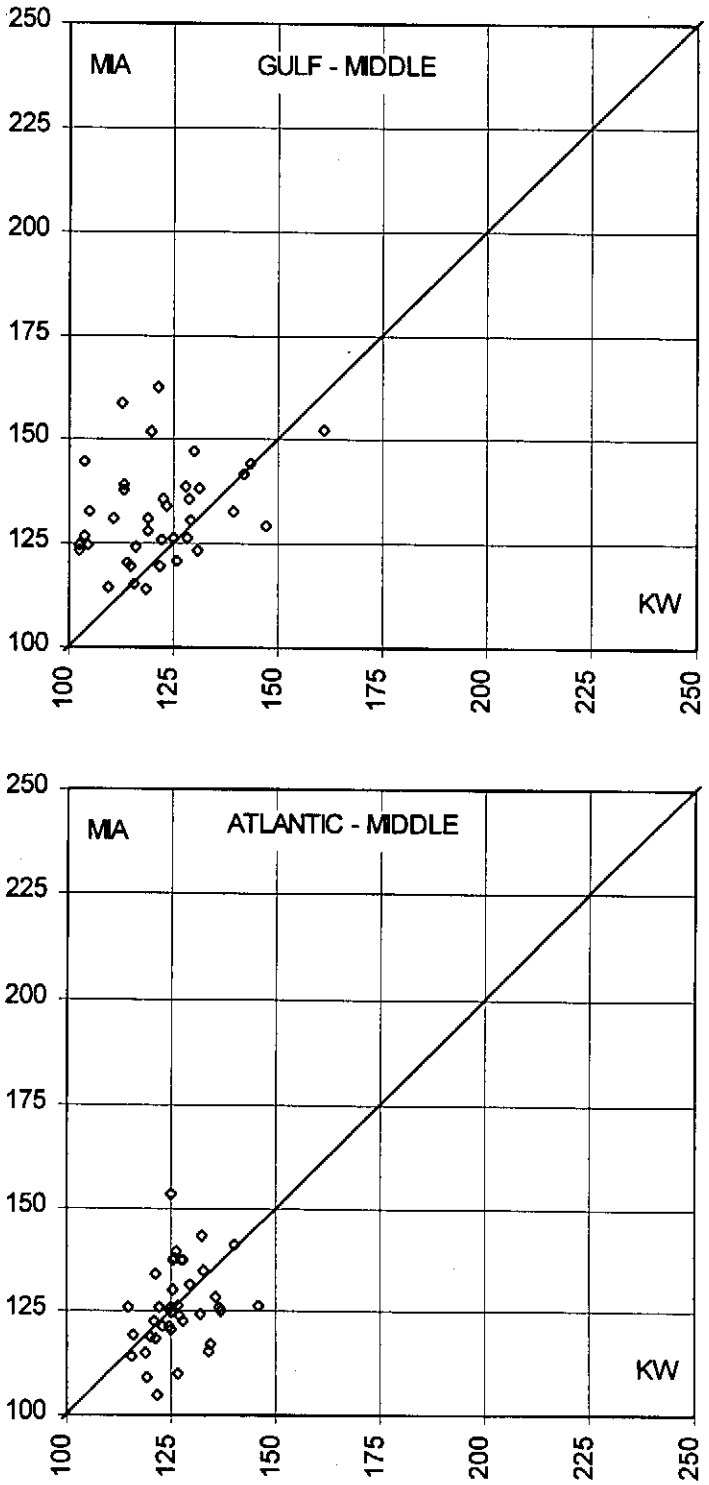

Figure 11. Calculated stiffness (kN-m^2) at the Miami end (MIA), as a function of the stiffness as the Key West end (KW), of each Middle tendon in the bridge. An ideal 1:1 diagonal line is shown for reference. The upper and lower graphs are for Middle tendons on the Gulf and Atlantic sides of the bridge respectively. The results shown are obtained using only the low frequency component of the double peaks.

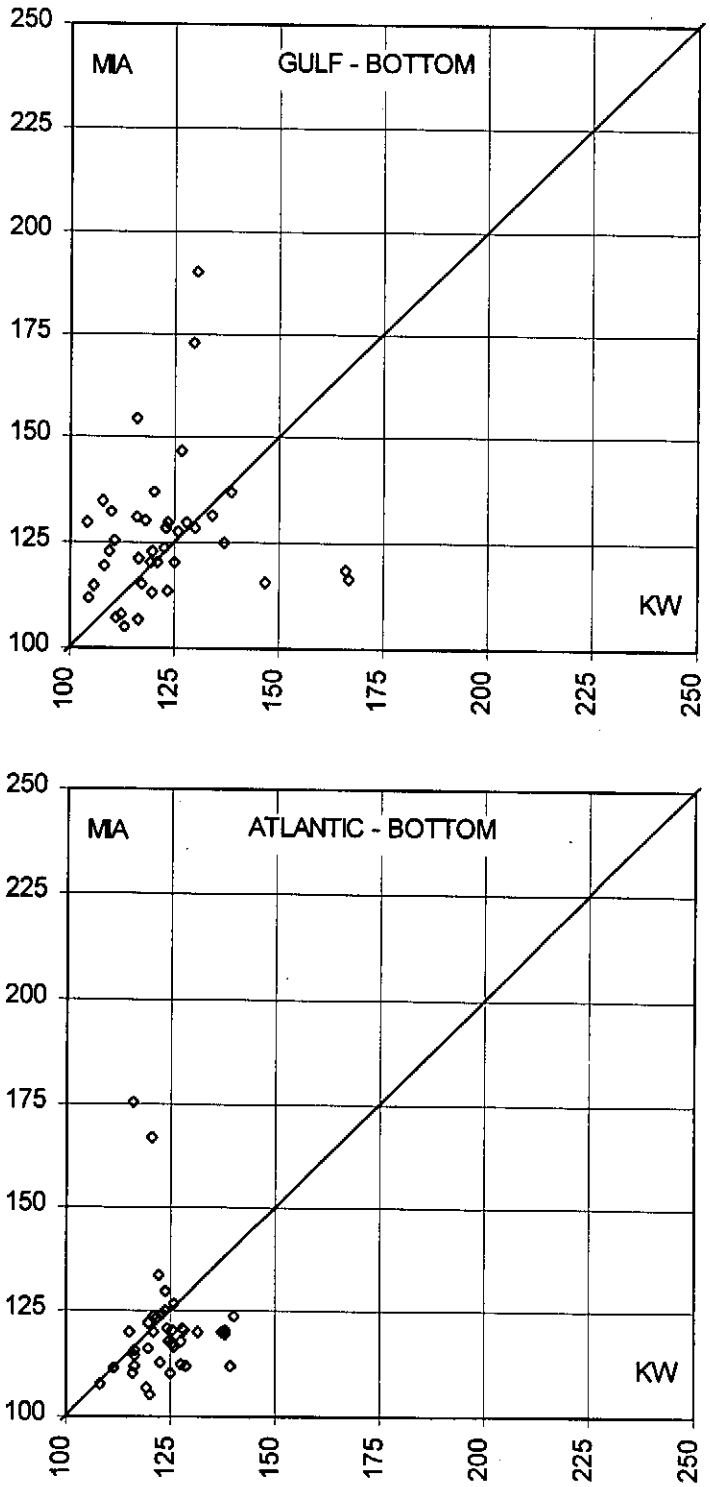

Figure 12. Calculated stiffness (kN-m^2) at the Miami end (MIA), as function of the stiffness at the Key West end (KW), of each Bottom tendon in the bridge. An ideal 1:1 diagonal line is shown for reference. The upper and lower graphs are for Bottom tendons on the Gulf and Atlantic sides of the bridge respectively. The results shown are obtained using only the low frequency component of the double peaks.

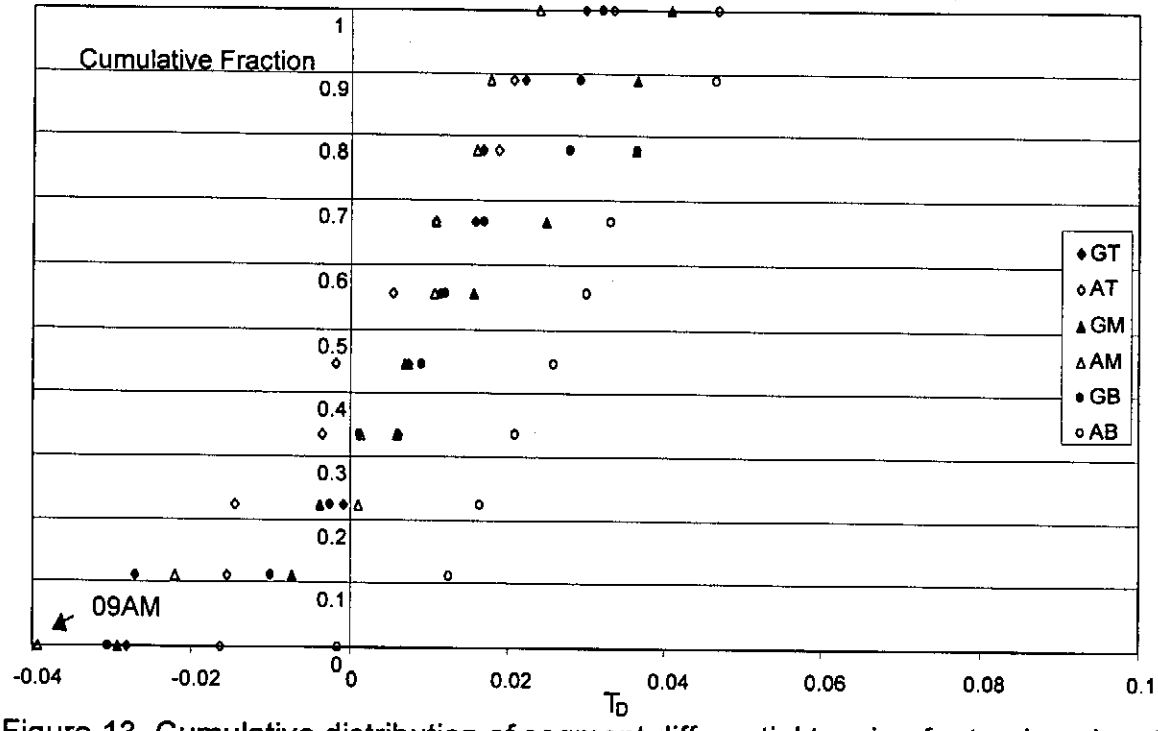

Figure 13. Cumulative distribution of segment differential tension for tendons located at expansion joints (T_D defined in text).

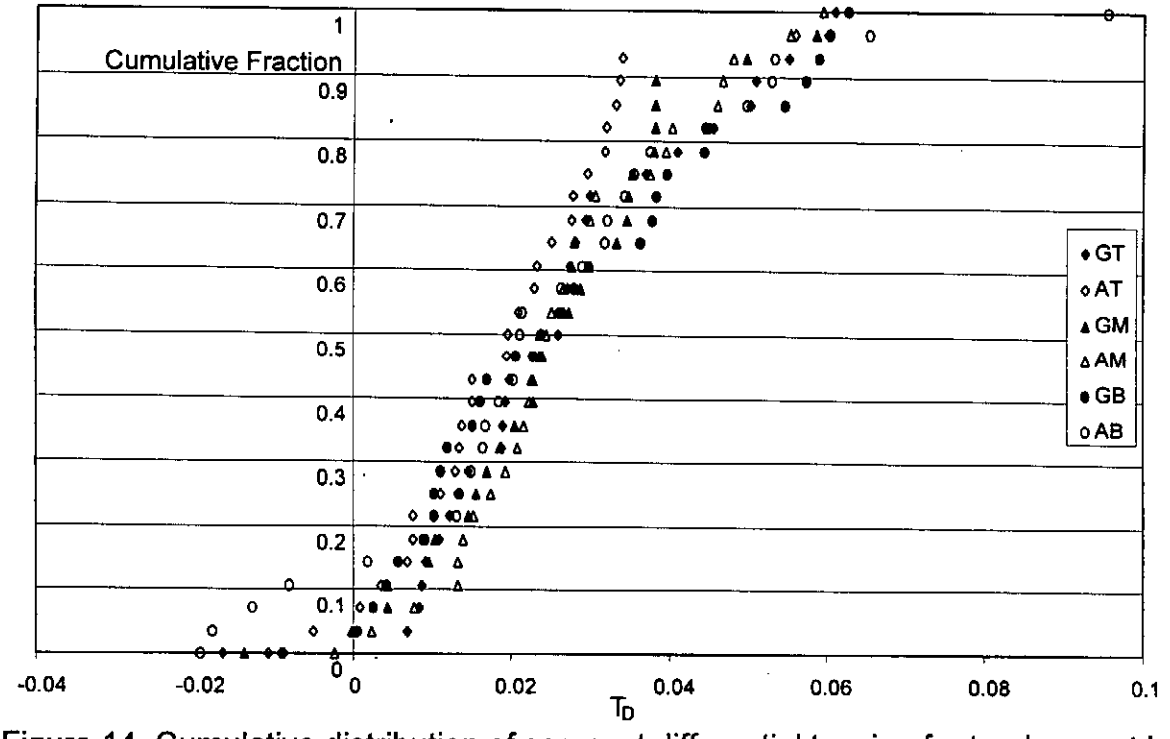

Figure 14. Cumulative distribution of segment differential tension for tendons not located at expansion joints (T_D defined in text).

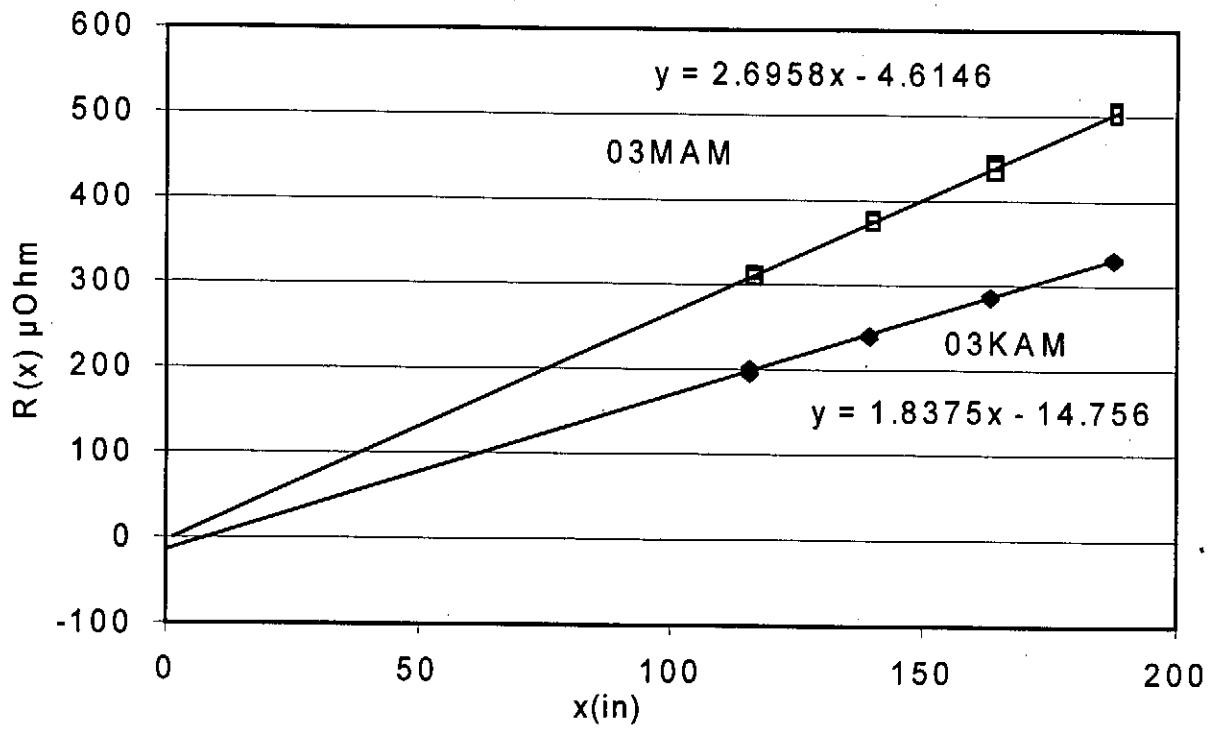

Figure 15. Example of electrical test results.

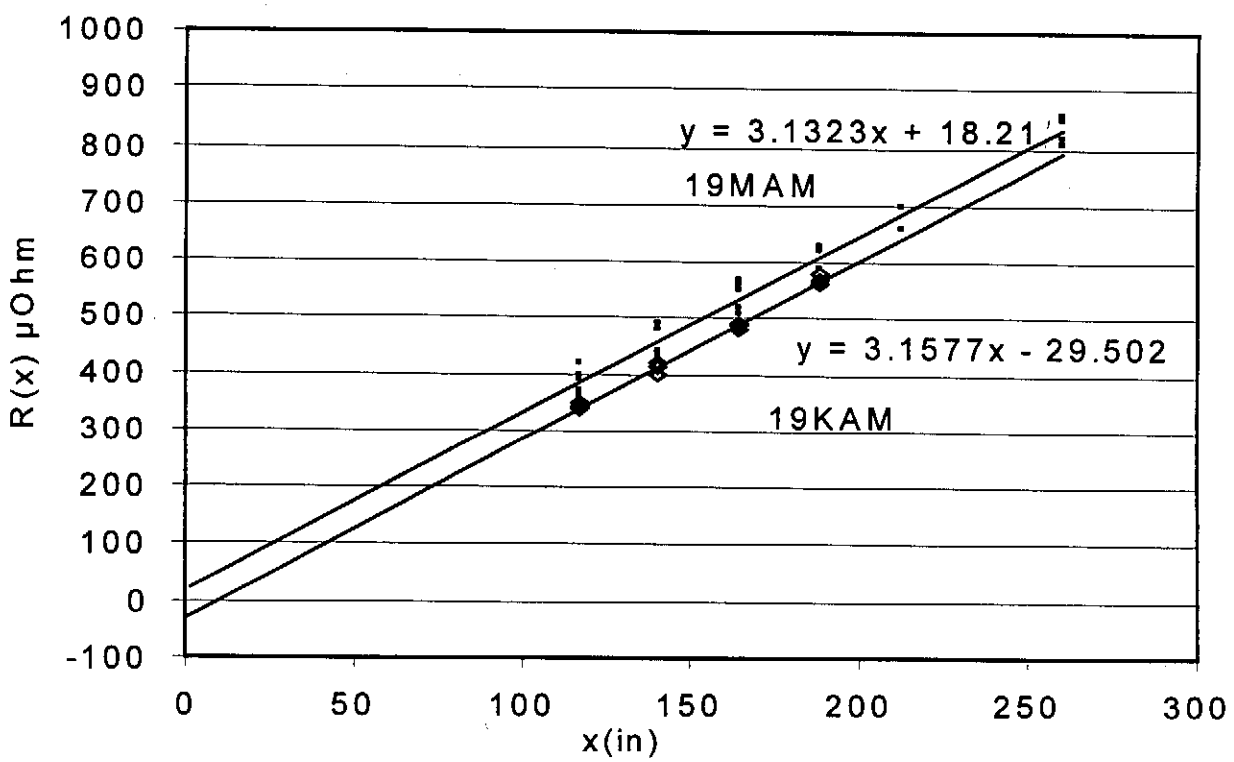

Figure 16. Example of electrical test results.

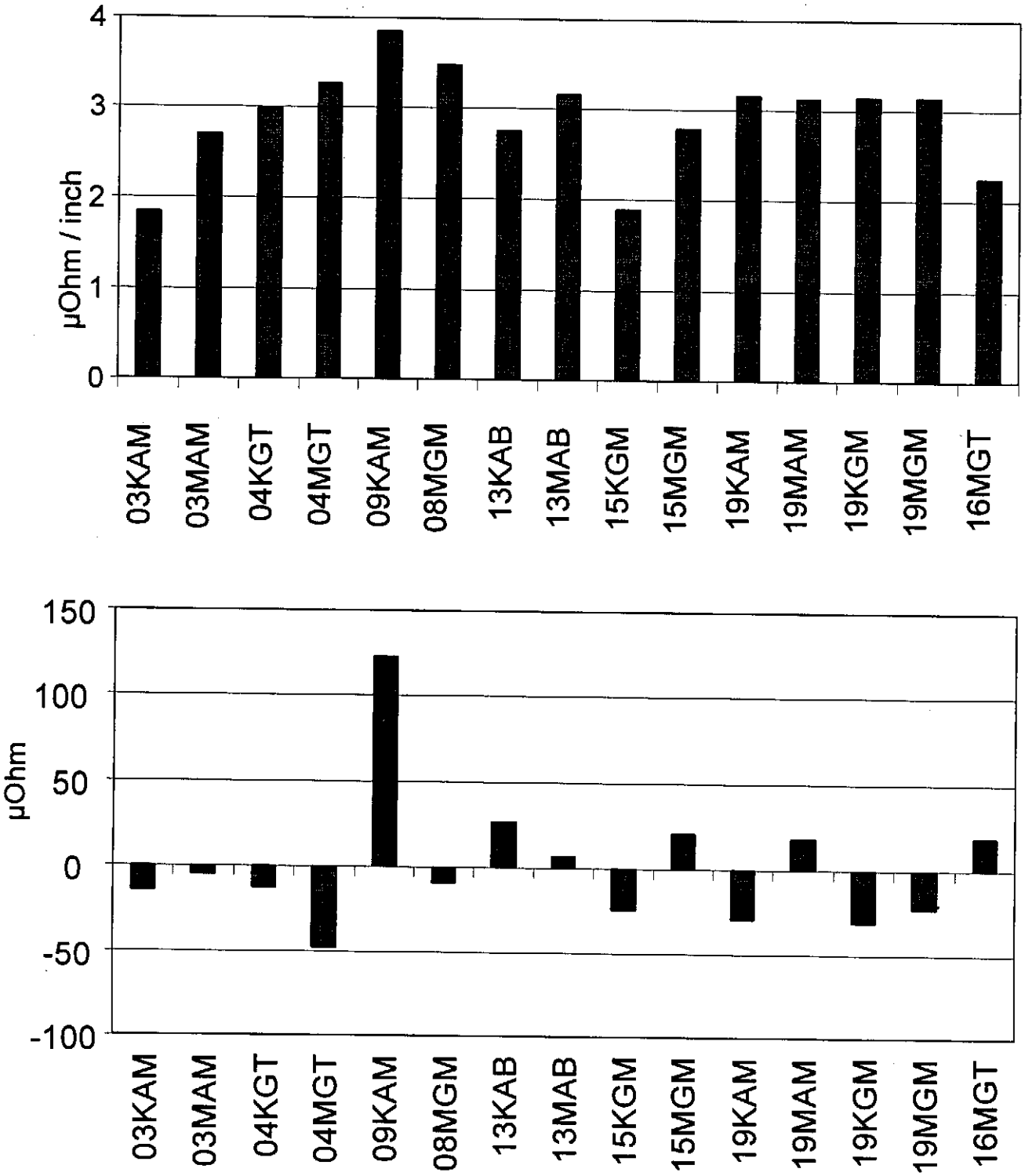

Figure 17. Summary of electrical test results (16MGT has 27 strands, all others 19 strands).